MODELLING AND ANALYSIS OF TUBE SPINNING

A THESIS SUBMITTED TO

THE GRADUATE SCHOOL OF NATURAL AND APPLIED SCIENCES

OF

ATILIM UNIVERSITY

BY

KEREM ÇİZMECİ

IN PARTIAL FULFILLMENT OF THE REQUIREMENTS FOR THE DEGREE OF

MASTER OF SCIENCE

IN

THE DEPARTMENT OF MANUFACTURING ENGINEERING

APRIL, 2017

Approval of the Graduate School of Natural and Applied Sciences, Atılım University.

Prof.Dr.İbrahim Akman

Director

I certify that this thesis satisfies all the requirements as a thesis for the degree of Master of Science.

Prof. Dr. S. Engin Kılıç

Head of Department

This is to certify that we have read the thesis "Modelling and Analysis of Tube Spinning" submitted by Kerem Çizmeci and that in our opinion it is fully adequate, in scope and quality, as a thesis for the degree of Master of Science.

Asst. Prof. Dr. Omer Music

Co-Supervisor

Asst. Prof. Dr. Caner Şimşir

Supervisor

Examining Committee Members

Assoc. Prof. Dr. Hakan Argeşo (ATILIM UNIV.)

Asst. Prof. Dr. Caner Şimşir (ATILIM UNIV.)

Asst. Prof. Dr. Omer Music (TED UNIV.)

Asst. Prof. Dr. Şehram Dizeci (TED UNIV.)

Asst. Prof. Dr. Eren Billur (ATILIM UNIV.)

Date: 26.04.2017

I declare and guarantee that all data, knowledge and information in this document has been obtained, processed and presented in accordance with academic rules and ethical conduct. Based on these rules and conduct, I have fully cited and referenced all material and results that are not original to this work.

Name, Last name: Kerem Çizmeci
Signature:

ABSTRACT

MODELLING AND ANALYSIS OF TUBE SPINNING

Çizmeci, Kerem

M.Sc., Manufacturing Engineering Department

Supervisor: Asst. Prof. Dr. Caner Şimşir

Co-Supervisor: Asst. Prof. Dr. Omer Music

April 2017, 69 pages

This thesis investigates the process of tube spinning. The investigation is based on numerical simulations by commercial finite element software Transvalor Forge. Two dimensional and three dimensional numerical analysis models have been developed. Parameter optimization has been performed to find the variables of numerical analysis. The proposed numerical model was compared with the related works in the literature. Using the developed models, analysis of tube spinning process has been performed.

Keywords: Tube Spinning, Finite Element Analysis, Modelling

ÖZET

BORU SIVAMA PROSESİNİN MODELLENMESİ VE ANALİZİ

Çizmeci, Kerem

Yüksek Lisans, İmalat Mühendisliği Bölümü

Danışman: Yrd. Doç. Dr. Caner Şimşir

Yardımcı Danışman: Yrd. Doç. Dr. Omer Music

Nisan 2017, 69 sayfa

Bu tez çalışmasında boru sıvama prosesi incelenmiştir. İnceleme ticari sonlu elemanlar yazılımı olan Transvalor Forge ile yapılan sayısal analizler ile gerçekleştirilmiştir. İki boyutlu ve üç boyutlu sayısal modeller geliştirilmiştir. En iyi sayısal analiz parametrelerinin bulunabilmesi için değişken çalışması yapılmıştır. Sayısal model akademik literatürde bulunan verilerle karşılaştırılmıştır. Geliştirilen modeller kullanılarak, boru sıvama proses analizi gerçekleştirilmiştir.

Anahtar Kelimeler: Boru Sıvama, Sonlu Elemanlar Analizi, Modelleme

To my family

ACKNOWLEDGMENTS

The author wishes to express his appreciation to his supervisors Asst. Prof. Dr. Omer Music and Asst. Prof. Dr. Caner Şimşir for their patience, advice and encouragement.

The author would also like to thank his current employer Nurol Makina ve Sanayi A.Ş. and previous employer Yüksel Kompozit Teknolojileri A.Ş. for their permission to perform his master education. Moreover he would like to say thanks to his colleagues for their support.

This study was supported by the Scientific and Technological Research Council of Turkey with the project ID 113M177.

TABLE OF CONTENTS

LIST OF FIGURES

LIST OF TABLES

CHAPTER

1 LITERATURE SURVEY

1.1 Introduction

The metal forming has been in the main focus of the industrial applications. Mechanical properties of formed products are better than the products manufactured by the other processes. Tube spinning has various application cases in the industry, particularly aviation and defense industry. Machine investment and try-our costs of the tube spinning process are expensive. Therefore, modelling and analysis of tube spinning have taken on an important role in both reduction of try-out costs as well as prediction of machine requirements and therefore the investment. Thus, finite element analysis method and simulation need to be applied for the tube spinning process. In this chapter, the definition of the tube spinning process is given and the literature review is presented. Literature review is categorized in to two groups that are experimental and finite element based approaches.

1.2 Definition of Tube Spinning

All metals cannot be used without having standardized for specific shapes. Therefore, they have to be machined, formed or cast. Many special manufacturing procedures are applied to the ingots in order to give desired shapes. Metal forming is one of the most advanced method that gives a shape to the metal. Lots of material forming processes are applied in metal forming area for instance rolling, forging, extrusion, and drawing. Additionally, there is a metal forming process that is named as “Tube Spinning”. Tube Spinning is an advanced manufacturing process that in the area of metal forming technology.

All metal forming processes include the forming by applying force to the workpiece. Tube spinning is also applied in this way; in tube spinning, rollers are used to apply force on the workpiece. The thickness is reduced and the length of the tube increases as it is deformed. Tube spinning process tools are mandrel, roller, tail stock, head stock as shown in the figure 1.1. Tube spinning can be applied in two ways that are forward and backward tube spinning.

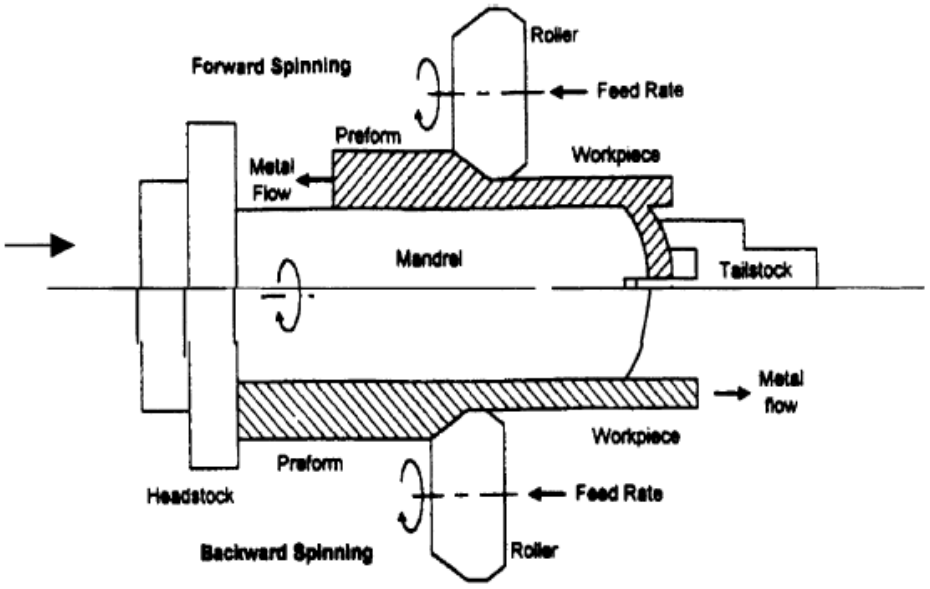

Figure 1.1 Forward and backward tube spinning (ASM Handbook, 1988)

Tube spinning has the following advantages:

- Mechanical properties (strength and quality) are improved
- High diameter to length ratio can be achieved
- Optimum grain flow
- Manufacturing without any chips
- Low tooling cost
- Good surface finish and high dimensional accuracy

In the literature, there exist related studies on the tube spinning technology. In the early studies, the tube spinning process can be considered as one of the initial approaches. The main process is metal spinning. Metal spinning comes from clay and pottery used in Egypt. Over time this is approach was applied in China, UK and USA. Today the process mechanism has also a similar structure. Workpiece and mandrel are rotating

and external forces are applied on the metal in order to shape it. Using spinning and tube spinning process, rotational axial symmetric parts can be manufactured easily, for instance, kitchen tools, musical instruments, car rims, defense industry parts etc.

Figure 1.2 Products manufactured by tube spinning

Tube spinning terminologies are shown in Figure 1.3;

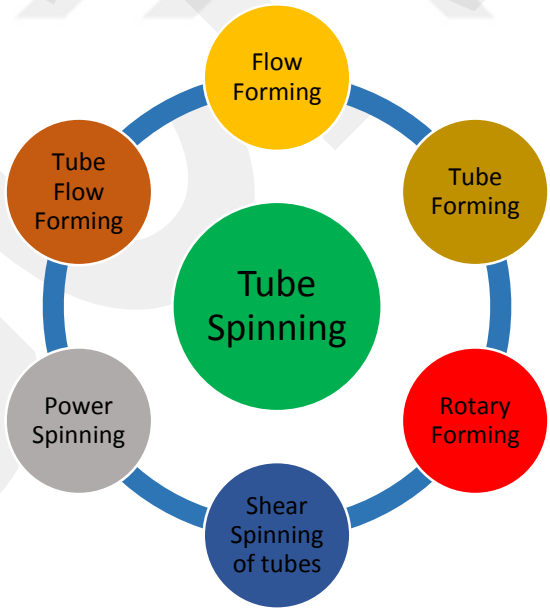

Figure 1.3 Tube spinning terminologies

During this study, tube spinning term is used. Shear spinning of tubes terminology comes from the shear spinning process due to shaping the tube with shearing. Rotary forming is used because all the bodies in the process have the rotational motion.

Deformed workpiece is an axisymmetric tube because of the usage of tube forming and tube flow forming.

1.3 Literature Survey

In this thesis, a number of articles in the research field of tube spinning have been reviewed. Regarding the spinning process, there exist a lot of certain results in comparison to the tube spinning technology. Although applying the tube spinning process is expensive and needs more investment for machines, many applied experimental approaches are available in contrast to the virtual experimental approaches. On the other hand virtual experiment has high computation costs because of the complex deformation mechanism.

1.3.1 Experimental Approach

Singhal et al. [2] made some experimental observations about shear spinning of long tubes. They used different materials such as pure Titanium, Incoloy and Inconel. They performed only experimental works on tube spinning. In their setup, they used forward tube spinning and two opposing forming rollers.

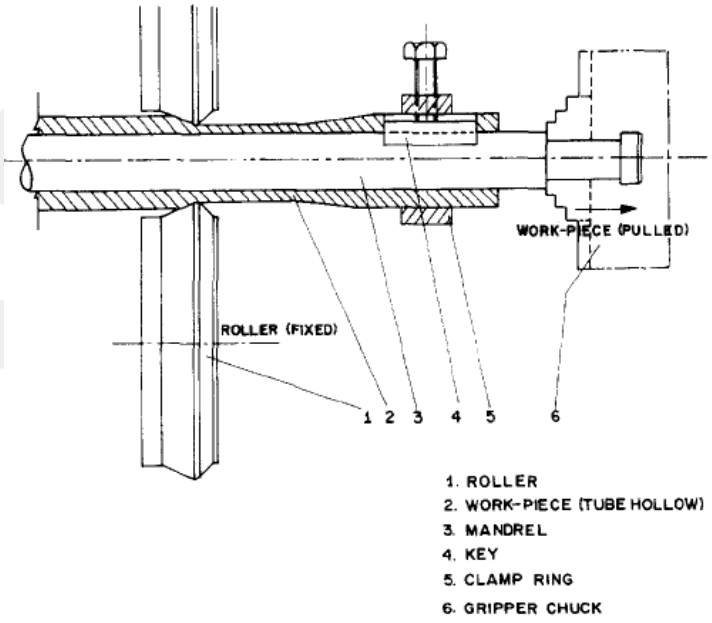

Figure 1.4 Tube spinning setup, [2]

As a result, they conclude that mechanical properties can be improved using the tube spinning process. Geometrical tolerances such as concentricity and surface finish are more sensitive than the other forming processes. They claimed that by increasing the reduction ratio, there is no appreciable change in micro hardness of the surface. However there is no information about process mechanism and mechanical properties of the formed metal.

Another study on the flow forming of cylindrical tubes was performed by Lee et al. [3]. Their approach is about how the average pressure on each roller changes according to frictional force between tube and mandrel. The results were supported through technical graphs. Number of rollers, roller geometry and their configurations were shown but process working principles and theory of the tube spinning process were not mentioned. Only force calculations were done by using sensors on the roller and mandrel. They found that the average pressure on the roller increases with frictional force between the workpiece and mandrel. On the other hand, they applied the back tension to the tube during process by a drawing die in order to reduce forces on the rollers. Forces on the rollers decrease with applied back tension. Back tension mechanism is shown in figure below:

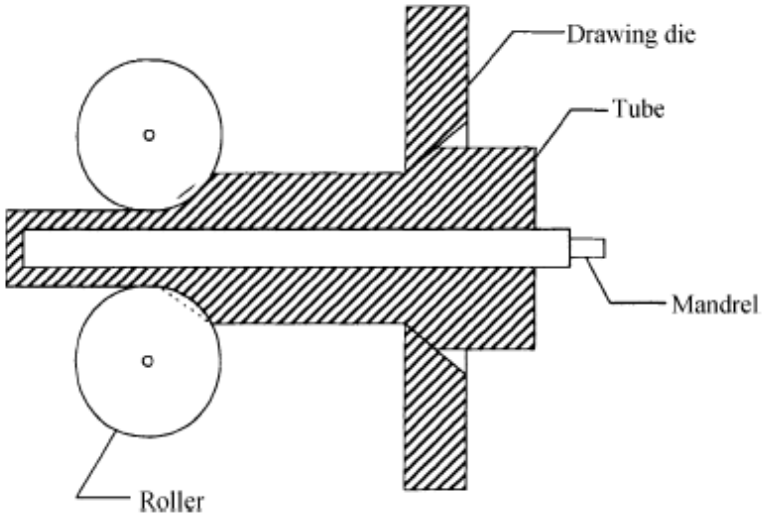

Figure 1.5 Back tension mechanism, [3]

On the other hand, Hayama et al. [4] made series of experiments for both forward and backward tube spinning processes. They examined the process in detail. All the process parameters, roller geometry and mechanical properties of the used material

were provided. Different roller angles, reduction ratios and feeding rates were used both forward and backward tube spinning process. Two opposite rollers were used to form of the tube. However, there is no information about the used rollers tip radius and friction coefficient. These two parameters directly affect the forces on the roller. For all experiments, rotation speed of the mandrel and system is constant.

Working conditions

Diameter of mandrel	d	mm	36
Diameter of roller	D_R	mm	74
Angle of roller	$\alpha=\beta$	deg.	15, 20, 30
Number of roller	n_0		2
Number of rotation of mandrel	N	rpm	210
Feed of roller	v	mm/rev.	0.124, 0.249 0.378
Thickness of tube wall	t_0	mm	2
Yield point of tube	σ_Y	kg/mm	23

Stress and strain curve of tube $\sigma=82\varepsilon^{0.251}$ kg/mm²

Figure 1.6 Process variables, [4]

Mild steel was used during experiments. Different feed rates were applied with different roller angles. Their effects on force of the roller which are tangential, axial and radial forces were examined and supported with detailed diagrams. Reduction ratio and radial force relation were examined, when reduction ratio increases, radial force on the roller will increase. The author claimed that there is a critical reduction value existing for both forward and backward tube spinning process. If the unsuitable feeding rate vs. reduction ratio values is used, the process gets the unstable condition. Critical reduction ratio values of forward tube spinning is less than the backward tube spinning for the same feeding ratio, it means that high reduction ratios can be applied by backward tube spinning process with high feeding ratios. Moreover, as roller angle becomes larger, higher feeding rates can be used.

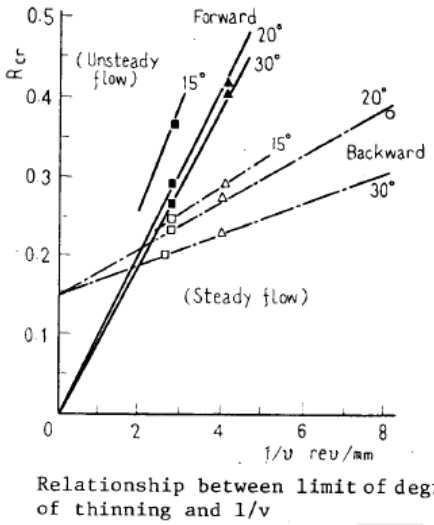

Figure 1.7 Critical reduction vs feed rate [4]

Author had not given any information about the length of the workpiece. This is important because length of the workpiece directly affects the forces on the roller. However, there is a graphic that includes the radial force, reduction amount and stroke of the rollers. Graphics had been drawn up to radial forces got the steady state condition. From this graphic, it could be predicted that stroke of the rollers were more than 30 mm.

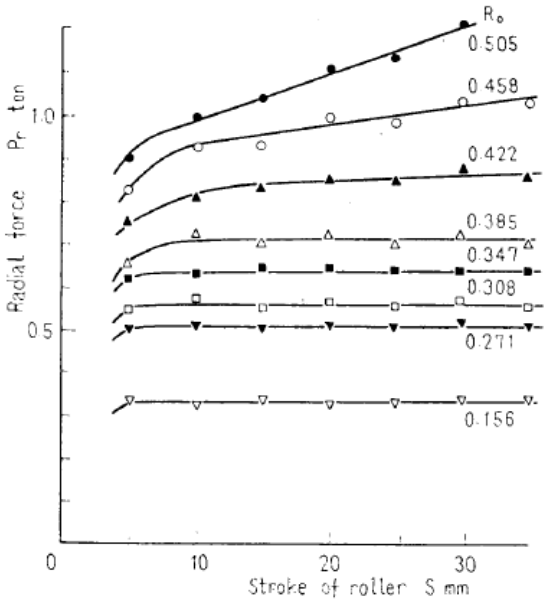

Figure 1.8 Radial force-reduction-stroke graphic, [4]

On the other, Hayama et al. [4] gave the information about reduction amount vs radial and axial force graphics for different angles of rollers. This force vs reduction amount graphics show the calculated results obtained by the theoretical methods.

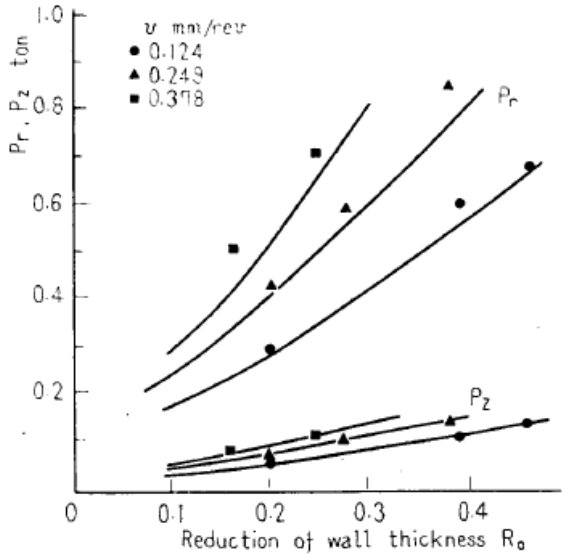

Figure 1.9 Forces on roller vs reduction graphic, [4]

So far, the researchers has been focused just on flat surface tube spinning. Groche et al. [5] developed a different type of flow forming process. Internally geared wheels were manufactured by flow forming. Special mandrel was used in their work. Mandrel has teeth on its surface and 3 rollers are applying the forces and deforming the tube.

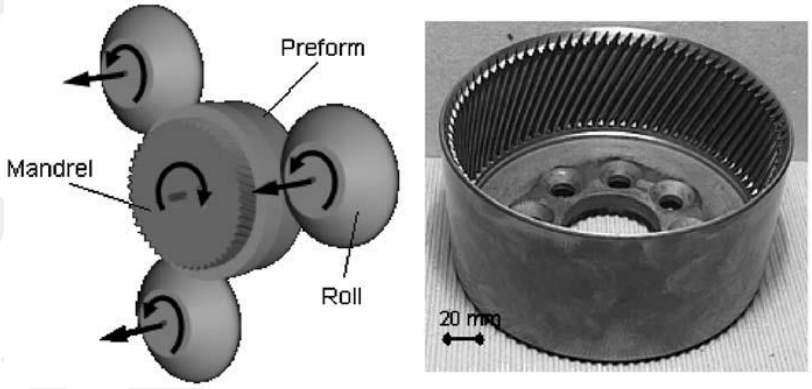

Figure 1.10 Three-rolls-principle and produced internally geared wheel, [5]

In the literature, this is a novel approach to tube spinning. Process is explained but detailed information was not given. Moreover, no modelling was done about flow forming via externally geared mandrel.

A review about tube spinning mechanism was done by Roy et al. [6]. Mathematical calculations and definitions are explained such as axial limits, maximum angular limits, iterative calculation of the contact length and contact area. Localized instantaneous deformation zone was pictured and explained in detail. Experimental

surface measurements of flow formed tube were done by FARO Laser Scan Arm and sensitivity of process analyzed.

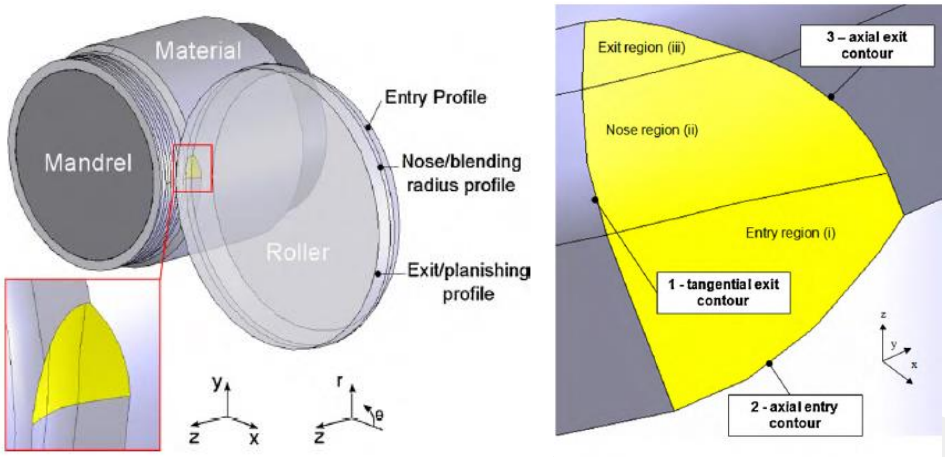

Figure 1.11 Detailed contact zone definitions, [6]

1.3.2 Research Done By Finite Element Method

Xu et al. [7] performed a 3D rigid-plastic FE simulation of tube spinning. In the model three rollers that were distributed with 120°, were used. The diameter of the mandrel was 70mm and 5mm thickness of the tube was used. In order to reduce the calculation time one third of the tube was modeled.

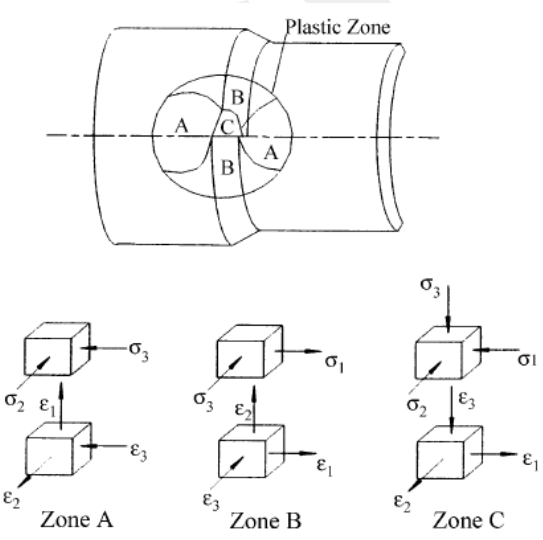

Figure 1.12 Schematic diagram of one third FEM, [7]

During tube spinning process, plastic zone occurs only about the roller's contact zone and it was separated into 3 different zones. The distributions of the stress and strain are very complex. They get stress and strain distributions, there is no difference

between forward and backward spinning. The deformation area can be classified according to the direction in radial, tangential and axial. However distribution of strains are not explained clearly. Moreover this is a one third model. Thus, a three dimensional model can simulate real tube spinning process closer to reality.

An analytical contact model for FEM was developed by Lexian and Dariani [8]. Flow forming process of a seamless pressure vessel was simulated. The shape of the final product is like a dome and it has nearly close edge. Only one roller was used and 8 increments were applied to form and to give a dome shape. When number of forming increments increases, the maximum effective plastic strain increases and mouth of the tube is more closed. Radial roller forces are greater than axial and axial roller forces are greater than tangential forces.

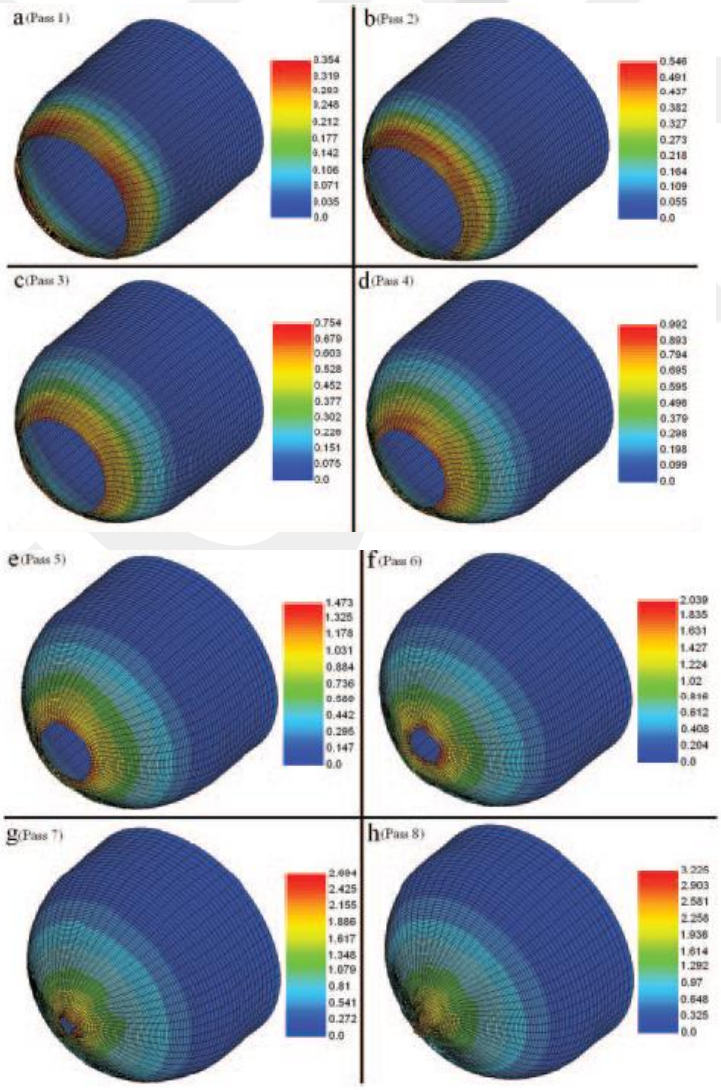

Figure 1.13 Dome shape forming by 8 increments, [8]

There is no table available about relation between flow forming rotational speed, most frequently used material and material thickness. Furthermore, there is not any information about which parameters have the most significant effect on the process. Moreover, this study is different from normal tube spinning process because of the final shape of the product.

Wong and others [9] investigated the effects of roller path and roller geometry on flow forming of cylindrical components. This is the most comprehensive research about tube spinning and process variables. They did both experimental trials and FEM analysis of the flow forming process. Two different roller types have been used flat type and rounded contact region which is named as 'nose' type as shown in Figure 1.14. When flat type of roller is used, metal moves predominantly along radial direction, forming flange. When rounded nose type of roller is used, metal flows predominantly along axial direction.

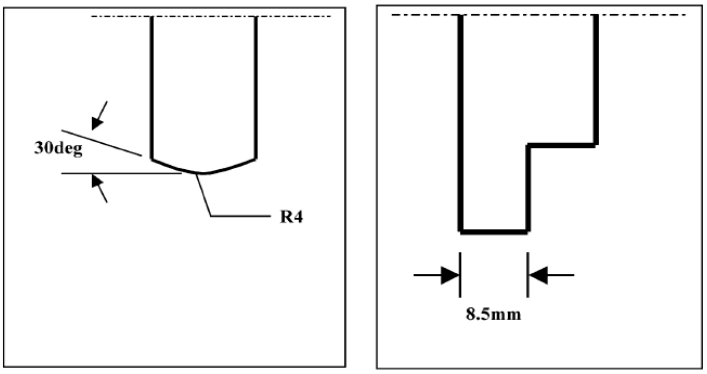

Figure 1.14 Different roller geometries, [9]

Many experimental results are available about roller types and roller pass direction. There is two roller path; first one is axial and second one is radial direction. There exists lots of comparisons about effects of roller types on flow formed products and the comparisons are supported via graphs. Furthermore, Wong and others made FEM model of process using ABAQUS and explicit 3D solid models. The work piece was meshed with 20416 8-node elements.

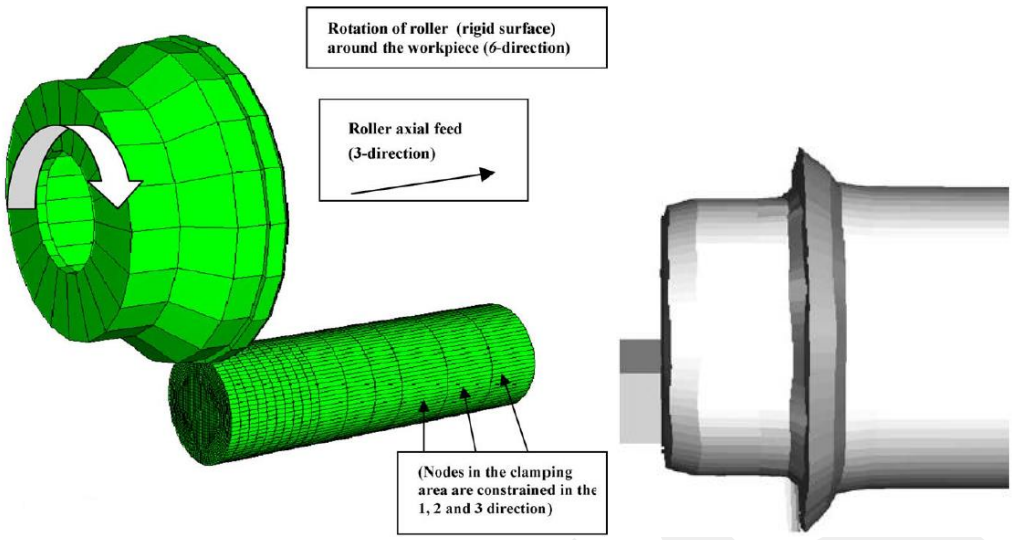

Figure 1.15 Numerical Model, [9]

Deforming region has a higher mesh density than the rest of the tube. However, in the model, workpiece is stationary in order to reduce computational time. The roller rotates around the tube, axial and radial movements. Therefore, this finite element method is different from real process, but approach gives an idea about deformation mechanism of tube spinning process. In the Figure 1.15, three dimensional finite element model is shown. Mesh density is higher at the deformation zone. Based on the simulations, the creation of flange is observed which can be seen at right side in Figure 1.15.

Hua et al. [10] worked on three-dimensional finite element analysis of Hastelloy C alloy. Three dimensional backward flow forming was simulated with ANSYS software. Three rollers were used for forming. Parameters of the entire process are defined in detail such as number of rollers and tip diameter of roller, rotation speed, feed rate, flow curve and material properties.

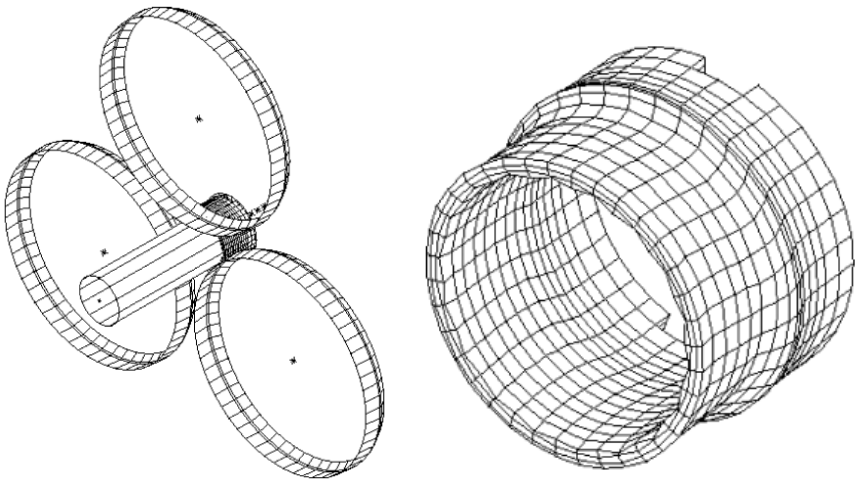

Figure 1.16 Three dimensional FEM backward tube spinning, [10]

Hua et al. [10] gave detailed information about deformation mechanism of backward tube spinning. Radial, circumferential and axial stress and strain distributions were given by visual aids. According to the results, authors claim that compressive stresses are on contact surface, and locally tensile stresses exist. Experimental results were verified by FEM results.

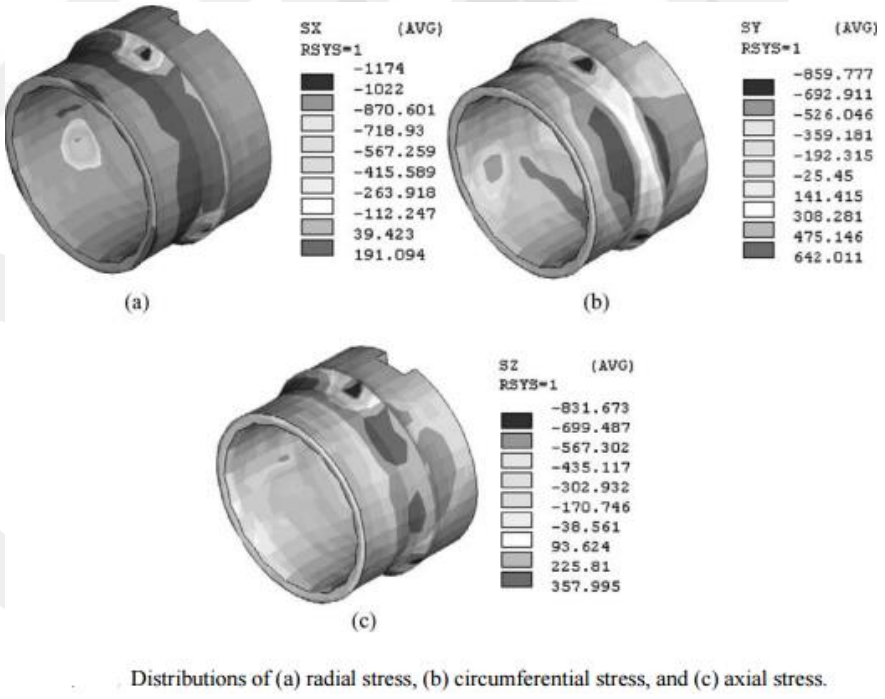

Figure 1.17 Stress distributions in cylindrical coordinates, [10]

Handong et.al [11] applied numerical simulation of tube spinning process by using metal forming software Simufact. Stainless steel DB. DIN.1.7242 was selected as raw material for the simulation. 3 different rollers were used and they were installed around circumferential direction with 120^{o} apart.

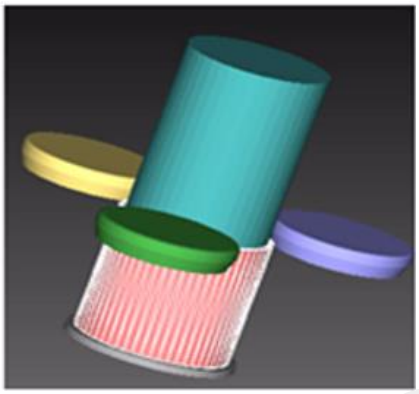

Figure 1.18. Process overview of tube spinning, [11]

Process parameters were explained in detail, thickness of the tube is 2 mm, length is 50mm and outer diameter of the tube is 50 mm. There is no information about mesh size and computational time. Handong and others [11] worked on temperature and effective stress distribution. They mentioned about basics of the tube spinning process.

Zhao et al. [12] worked on hot power backward tube spinning process. Aluminum 7075 series was selected as a raw material for simulations. They based on the platform ABAQUS /Explicit model. They analyzed the effect of the thinning rate and preheating temperature on bell mouth in tube spinning process. They worked on reduction ratio vs preheating temperature proportion. They claim that as reduction ratio increases, preheating temperature value increases.

Ma et al. [13] were interested in maximum thickness reduction ratio of the tube spinning process. However, it is not easy to predict reduction ratio limits of tube spinning process because of tube spinning process' complexity. They aimed to select appropriate ductile fracture criteria. During their studies, ABAQUS software and its ductile fracture definitions were used for TA2 titanium.

1.4 Conclusion of Literature Survey

While there are no comprehensive and descriptive examples made with numerical methods related to tube spinning in the literature, much experimental research is available. As the day-to-day approaches, a reduction in the number of experimental studies is observed. The parameters used in experiments are most clearly described in the reference number [4].

2 TWO DIMENSIONAL MODELLING

2.1 Introduction to Two Dimensional Modelling

In this thesis, experimental results from Hayama's studies [4] were taken as a reference and been modelled with finite element method. Forward tube spinning process is simulated. Two independent rollers and one mandrel were used during experiments. Hayama et al. [4] tried 3 different roller type, rollers were grouped according to their back and front angles which are 15°, 20° and 30°. Back angle and front angle are denoted by α and β. On the other hand, different feeding rates were tested for tube spinning experiments in papers [4], which are 0.124 mm/rev, 0.249 mm/rev and 0.378 mm/rev. Mandrel has a rotation speed 210 rpm and its converted rotation speed is 3.5 rev /s. The determined parameters of Hayama et.al. [4] and their symbols are presented in Table 2.1.

Table 2-1 Parameters used by Hayama

HAYAMA'S EXPERIMENTS CONDITIONS	Parameters	Symbol and units	Values
	Diameter of mandrel	d (mm)	36
	Diameter of roller	D_R(mm)	74
	Angle of roller	α = β (deg)	15 , 20 , 30
	Number of roller	n_o	2
	Rotation of mandrel	N (rpm)	210
	Feed of roller	v (mm/rev)	0,124 , 0,249 , 0,378
	Thickness of tube wall	t_o(mm)	2
	Yield point of tube	σ (kg/mm)	23
	Degree of thinning	R_o or R_{cr}(mm)	0.2 - 0.57

In the paper [4] there is no information about the tube length. However, graphics give clues on the tube's length. For instance, radial force of roller – roller stroke graph (in Figure 1.8), roller stroke axis is drawn up to 30 mm. After a point radial force on the roller gets the steady state condition, it will not change up to process end. The result is that tube's length is more than 30mm. Therefore, for two dimensional finite element model, the tube length is estimated as 100 mm.

The scope of the tube spinning simulation and modelling is explaining to the process mechanism. Firstly two dimensional tube spinning simulation modelling is performed in order to interpret about mechanism of the process and the roller forces. Tube spinning operation has a structure that is an axial symmetric geometry. During deformation, spun material has to be gathered in front of the roller, this situation is named as wave formation.

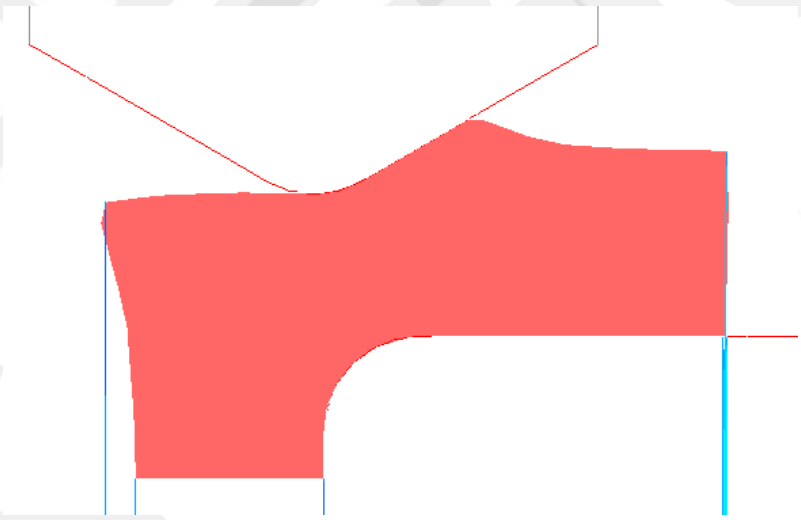

Figure 2.1 Wave formation in front of the roller

Shape of the wave depends on many parameters that are material type, feeding rate of the roller, degree of thinning or reduction ratio, roller angles. Because of the gathered material in front of the roller, rollers are under loading and resistance that depends on the size of the wave. In an axisymmetric geometry, cylindrical coordinate system is used.

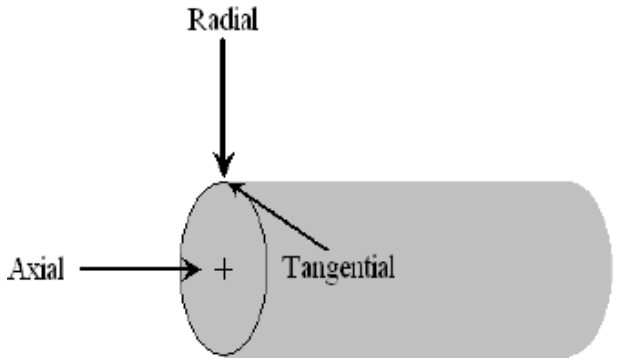

Figure 2.2 Axisymmetric Structure's Coordinate axis

During the tube spinning process, 3 different forces occur on the roller. These forces are along tangential, axial and radial direction.

- F_θ is used for tangential force.
- F_z is used for axial force.
- F_r is used for radial force.

As a hypothesis, during process there is a point that after roller passes it, radial forces on rollers get the steady state condition, it does not change until the process end. Radial force can be separated in 3 steps; at the beginning of the process radial force is increasing. At the second portion it is getting a steady state condition and finally it is decreasing. In order to observing and demonstrate this situation two dimensional modelling is the easiest method. Because three dimensional modelling takes too much time for instance; when a tube that is 60 mm length and 40 mm and 38 mm outer and inner diameter, is modelled and analyzed, it will cost several days in a finite element software. However, in order to understand the process mechanism three dimensional modelling has to be done even if it is going on long. Thus in two dimensional model, wave formation and flaring mechanism cannot be observed.

2.2 Two Dimensional Modelling of Tube Spinning Process

For two dimensional model, Transvalor Forge NXT version 1.0.2 commercial finite element software is used. In tube spinning process, workpiece and mandrel are axial symmetric geometries. Therefore only half of the cross section has been modelled. During the tube spinning process, deformation localizes under the rollers. Therefore, deforming tools have localized contact area with workpiece. Contact areas depend on

tip radius of the rollers. Because of the tip radius, there is an ellipsoid contact area occurs on the work piece, presented in Figure 2.3:

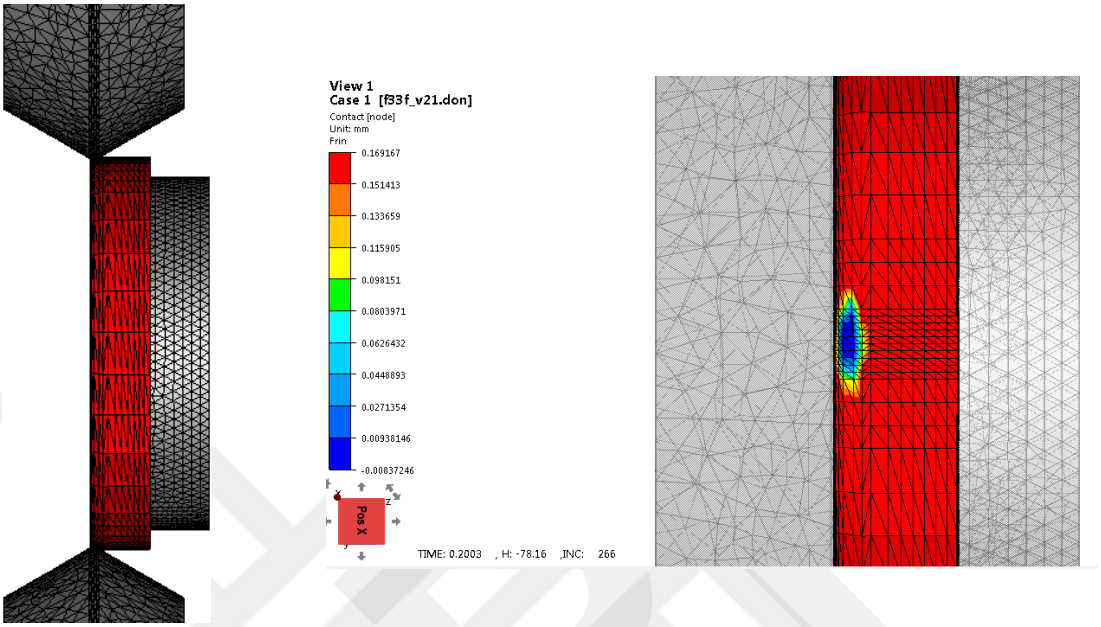

Figure 2.3 Contact area of the roller on the tube

However, when two dimensional analysis is performed, roller behaves as fully contact with the deformed region. Hence, while calculating the radial forces that act on the roller, pressure should be divided with the ellipsoid contact zone area.

2.2.1 Mechanical Properties of Used Material

In two dimensional finite element analysis models, Hayama's parameters [4] have been used that are, mandrel and tube diameter, tube thickness, roller diameter, feeding rate of roller and material type. Hayama et al. [4] used a cylindrical blank machined from a commercial mild steel work piece that has a flow curve equation; $\sigma = 804.42 * \varepsilon^{0.251} N / mm2$ and steel's yield point is 225,63 MPa, steels mechanical properties was obtained from a compressive test done by Hayama. The same material is used in all two dimensional and three dimensional analysis during this study.

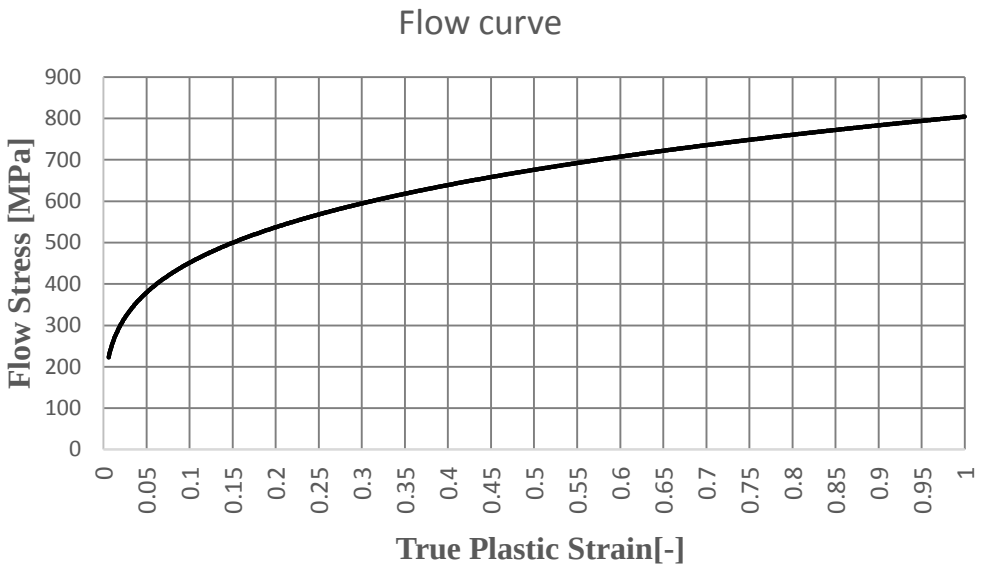

Figure 2.4 Flow curve of used steel

2.2.2 Two Dimensional Model Parameters

From two dimensional analysis elongation can be predicted. Moreover, it gives much information about deformation mechanism of the tube spinning process. Hayama et al. [4] did not give any information about the tube's length. In tube spinning mechanism, rollers translate only axial direction and they are free to rotate around themselves because of frictional force. For two dimensional analysis, a tube that has 60 mm length, 40mm outer diameter, 2 mm thickness is used. Roller angle is 30^{o} and 0.25 mm mesh size is used and remeshing is activated for the all process. Reduction ratio is % 0.25. Tube, mandrel, roller and plate manipulator are modelled as axisymmetric along the horizontal "z" axis in Figure 2.5.

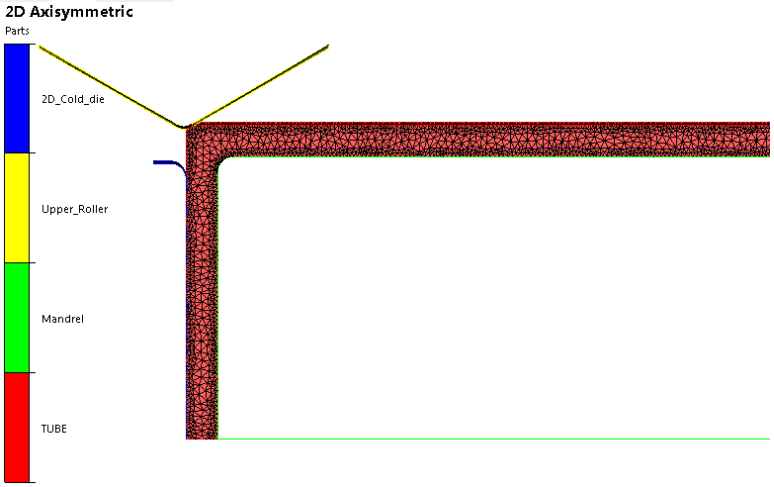

Figure 2.5 Two dimensional FEM Model

Two dimensional finite element analysis gives idea about process mechanism, strain and stress distribution along radial, axial directions and force on the roller. During the deformation flowed materials pile up in front of the roller, and this situation is referred as “wave formation“. Observing the wave formation is not possible in two dimensional finite element analysis. Because of axisymmetric assumption, deformation along the circumferential direction is assumed to be zero.

2.2.3 Strain Rate in Two Dimensional Model

During deformation, when strain rate is examined, it is obvious that the largest deformation occurs on the tube surface but deformation can reach towards to the radial direction of the interface between the tube and mandrel because of these situation tube‘s length elongates. Additionally, strain rate gives instantaneous information about the deformation.

If the strain rate is observed, deformation can reach to the bottom surface of the tube and this can explain the mechanism of the tube spinning and why tube elongates. Strain rate and instantaneous deformation is shown in the Figure 2.6.

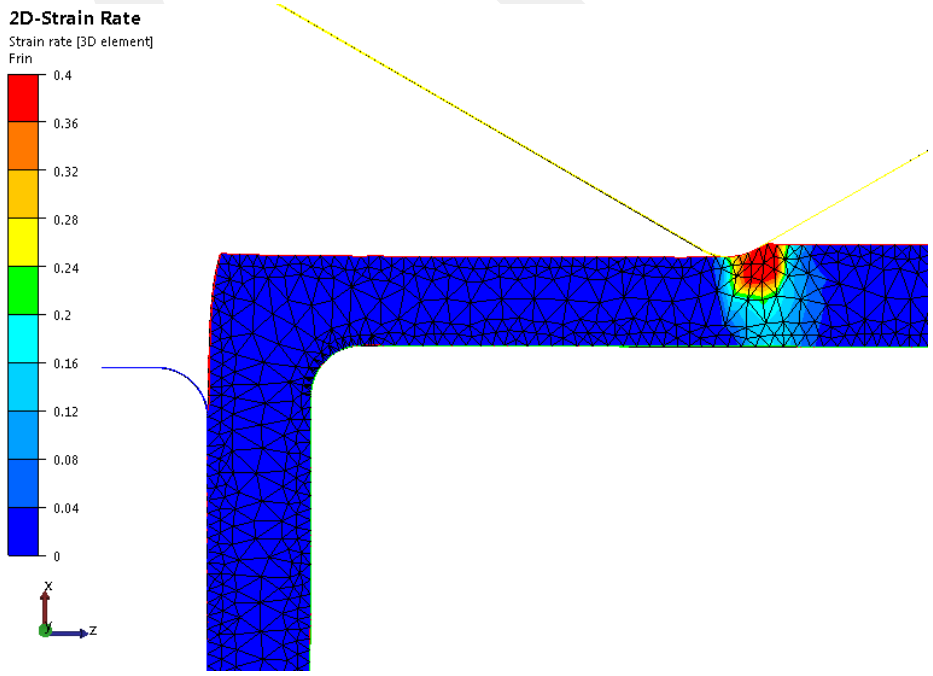

Figure 2.6 Two dimensional FEM strain rate distribution

Deformation penetrates up to inner surface of the tube, slipping occurs and tube elongates. Strain rate values in outer surface of the tube are higher than the inner surface values, therefore outer surface is deformed more than the inner surface. Moreover, it is not zero at inner surface.

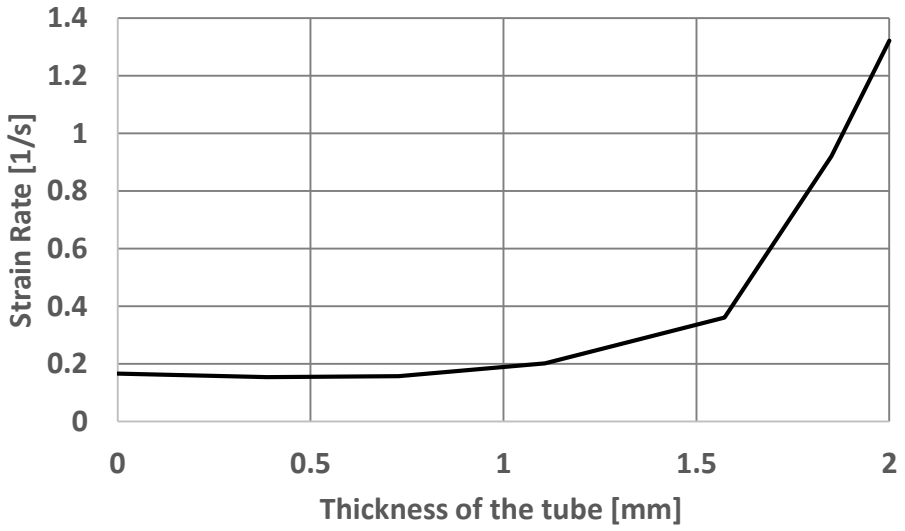

Figure 2.7 Strain rate distribution from inner to outer surface for 2D analysis

2.2.4 Axial Non-Uniform Growth Formation

Elongation of the tube continues homogenously up to a certain time. However, as roller comes to the end of the tube, outer surface of the tube elongates faster than the inner surface and deformation localizes on the upper surface, it is shown in Figure 2.8; strain rate of the outer surface is more than inner surface Another reason of this situation is frictional force at inner surface is more than the outer surface. Frictional force holds to material at inner surface and not allowed to elongate more. At the end of the process, the strain rate of the upper surface is more than the bottom surface and deformation vector cannot react up to the inner surface. Therefore, upper surface elongates faster, which is named as **"axial non-uniform growth formation"**. After process finished end of the tube should be cut to get the homogeneous elongated tube.

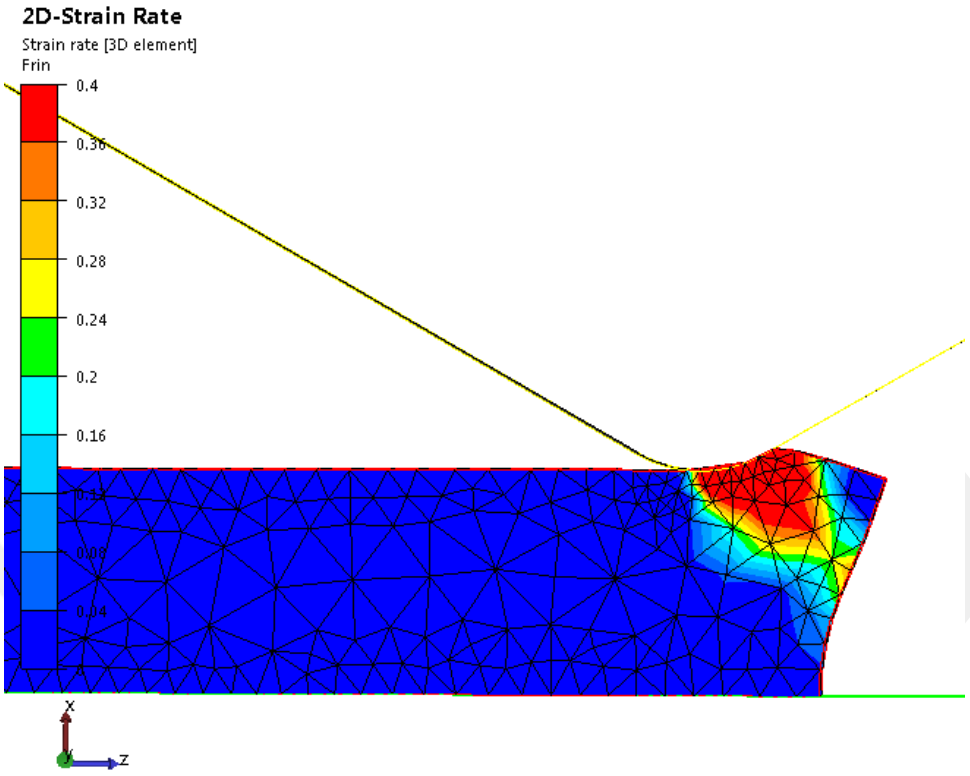

Figure 2.8 Axial growth in 2D FEM

2.2.5 Force on the Roller in Two Dimensional analysis

Rollers carry forces which are along the radial, tangential and axial direction. When radial forces are examined, after a certain point radial force on the roller becomes constant for a certain interval. This is a unique property for tube spinning process. Because of these steady state condition for radial force, there is no need to model the tube up to last, just a part of its length is enough to get information about the deformation and forces. This is proven with 2D tube spinning analysis; after a point radial force on the roller is getting a constant value as shown in Figure 2.8. Force along radial direction on roller is about 10 tones and it is constant up to the end of the process.

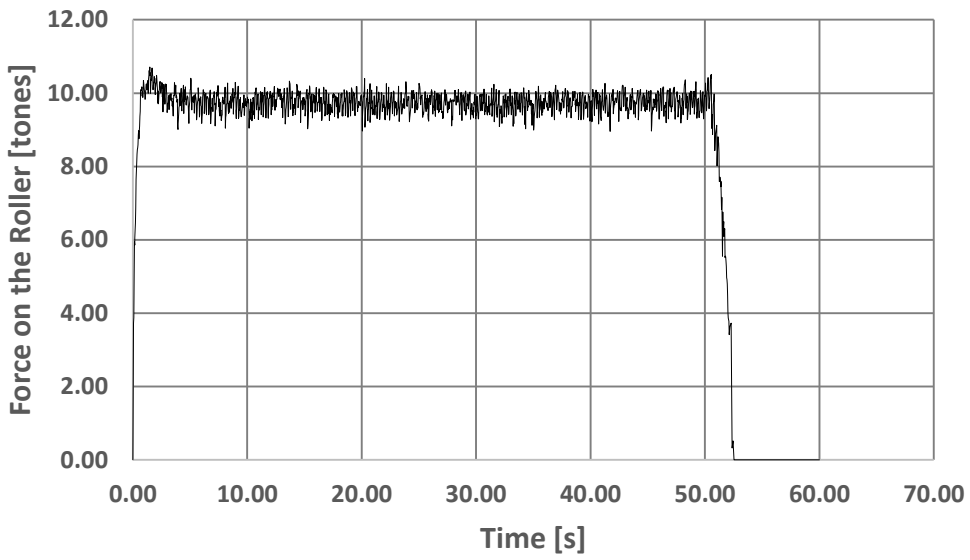

Figure 2.9 Force on the roller in 2D analysis

Forces on the roller are directly proportional with the reduction ratio of the thickness and feed rate of the roller, as they increase, forces on the rollers will increase. During the tube spinning process, reduction ratio and feed rate are constant. The process is getting to steady state condition after a point and force do not change during the process for a certain time interval. There is no need to simulate a long tube, for instance, by using a half model, same results with the full model can be observed. At this point, contact pressure on the rollers can be compared between two dimensional modeled analysis and three dimensional modeled analysis. During tube spinning process rollers contact just a small area like an ellipsoid in three dimensional loading as shown in figure 2.10.

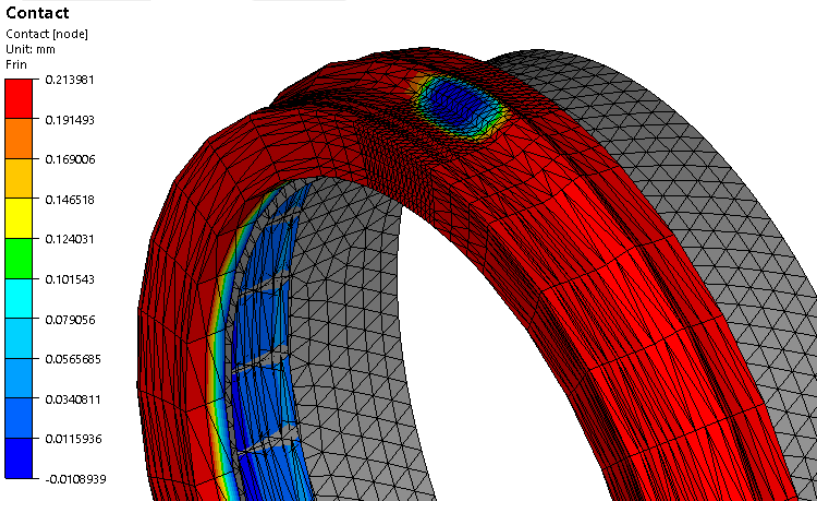

Figure 2.10 3D view of roller contact zone

This ellipsoid surface area can be calculated approximately as shown below, major and minor axis lengths of contact zones are about 4.83 mm and 2.12 mm. In two dimensional analysis, when the force towards to the roller is divided with this area, contact pressure on the roller can be calculated.

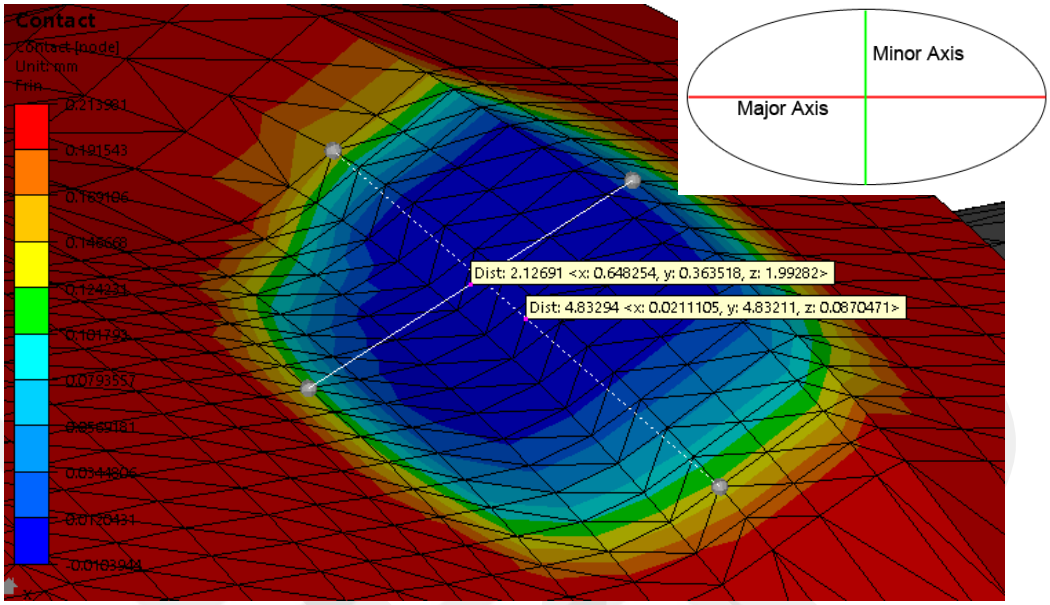

Figure 2.11 3D ellipsoid contact zone

$$A_{ellipsoid} = \frac{\pi * a * b}{4} = \frac{\pi * 4.83 * 2.12}{4} \Rightarrow A_{ellipsoid} = 8.042 mm^2$$

Maximum pressure on the contact surface is about 800MPa and area of the ellipsoid contact zone is 8.042 mm^2. $\cos\alpha$ is the angle of the roller.

$$\sigma(MPa) = \frac{Force(N)}{Area(mm^2) * \cos\alpha} \Rightarrow 800MPa = \frac{F}{8.042mm^2 * \cos 30} \quad F = \frac{5571.6}{9.81 * 1000}$$

$$F = 5571.66N \qquad F = 0.56 tones$$

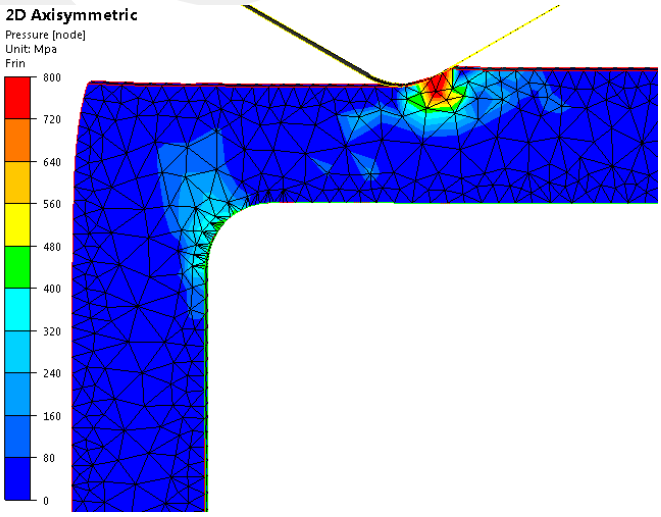

Figure 2.12 Pressure on two dimensional model

Force graphics can be compared with the Hayama's angle of roller vs force graphics. Hayama represented the tangential, axial, radial and total force with the symbols P_{θ}, P_z and P_r. When Hayama's roller angle vs resultant force graphic is examined, force is between 0.5 and 0.6 tones as shown in Figure 2.13. From two dimensional results, force is calculated from roller's ellipsoid contact area and it is calculated as 0.65 tones. Hayama's resultant force and calculated force from pressure are nearly close to each other

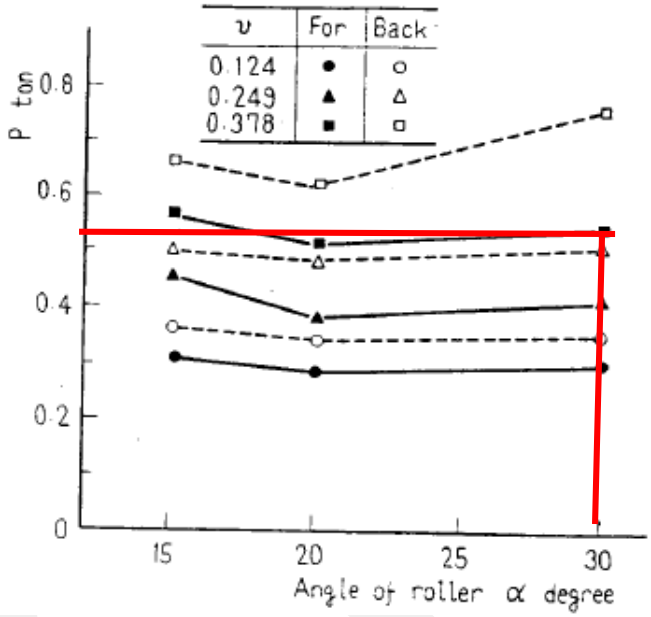

Figure 2.13 Total force vs angle of roller graphic [4]

2.3 Conclusion of Two Dimensional Analysis

As a result, two dimensional finite element analysis just give an idea about the total force on the roller .Therefore, if total force would like to be calculated in detail and other components, three dimensional analysis has to be done. On the other hand, as rollers feeding velocities increase, radial forces increase and as reduction level increases, radial and axial forces increase because wave grows and resists to the deformation towards to the roller. It is obvious that, in tube spinning process, deformation concentrates under the roller, and it can affect up to contact zone between the mandrel and tube. Before performing the experiment, it can be predicted that forces are enough to deform all material along thickness or not and if deformation localizes on the surface and elongation velocity of the surface is larger than bottom surface. As a result of this non uniform axial growth occurs end of the tube.

3 THREE DIMENSIONAL MODELLING

3.1 Introduction to Three Dimensional Analysis of Tube Spinning Process

Tube spinning process has a complex stress distributions during forming. In order to understand mechanism of the process, three dimensional model should be used. In this chapter, Transvalor Forge‘s special structured ring mesh method is used to model the process and reduce computational time. On the other hand, two different remeshing box approaches are trialed. Finally, optimum mesh size parameter study is explained.

3.2 Structured Ring Mesh Theory

In order to reduce the computational time, a special mesher has to be used for 3D simulation of the tube spinning process. Transvalor Forge has a specific solution approach for this purpose - structured ring mesh.

In general, the meshes used in the software are unstructured. It should be noted that there is an exception for tube spinning simulation in which the mesh is necessarily structured in the ortho-radial direction. A sample of ring mesh is shown below.

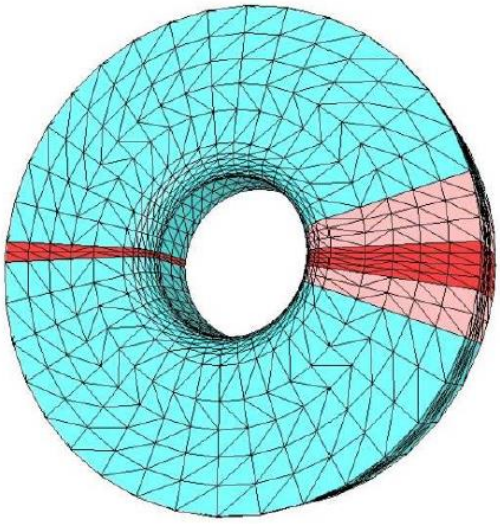

Figure 3.1 A sample of structural ring mesh

A specific mesher is used to generate the structured mesh from a ring that has been freely volume meshed. This ‘structured ring’ mesher works according to a two-stage process: It starts by meshing a slice of the ring (Figure 3.2 - a). This slice is duplicated by a circular symmetry centered in the center of the ring and according to an angular pitch that is defined by the user. Each triangle in the slice created is then connected to its downstream neighbor to create 3D prisms (Figure 3.2 b). After that, these prisms are discretized into 5 tetrahedrals. Repeating this operation over 360° will generate a structured and circular discretization of the ring. If the initial ring is not perfectly circular, once meshed, it will be projected onto the initial geometry. Therefore, while importing a three dimensional model to the software forge, it should be well prepared and fine meshed for the STL format. Volume meshes are created by referenced imported STL file. If the imported STL meshes are coarse, ring roundness will be distorted.

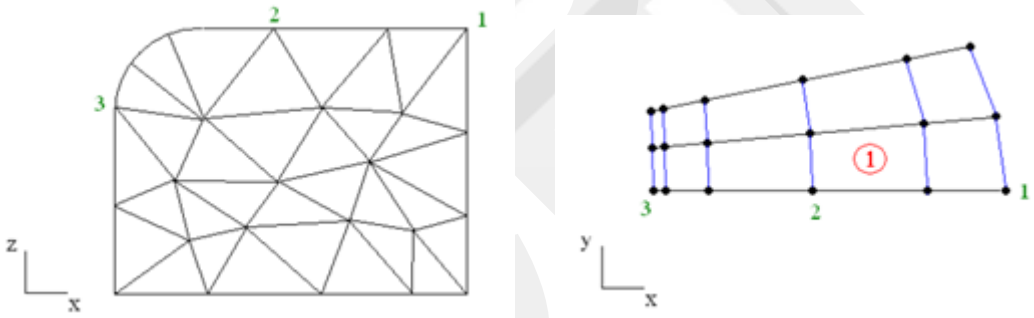

a) b)

Figure 3.2 a) 2D unstructured slice, b) 2D extruded slice

In the case of tube spinning process, the structured ring meshing method very significantly reduces computation time by preserving a fine mesh in the useful area only while significantly reducing remeshing operations.

3.3 Mesh Size and Remeshing Approach

In this section two different remeshing box approaches are mentioned. Mesh size parameter study is performed with different remeshing approaches. Force, strain rate, computational time and von Mises stress comparisons are explained.

3.3.1 Full Length Cylindrical Remeshing Box

In order to decide which size of tube mesh is useful for 3D modelling, 3 different mesh sized simulation were performed. Each of them has the same remeshing box to decrease the computational time. For three dimensional analysis 30° front and back angled rollers were used, for the feeding rate 0.378 mm/rev was used. The force is applied by 2 rollers that are positioned around the tube at 180° angles. These 3 analyses parameters are shown in the table below.

#	Simulation Name	Roller Angle	Feeding Rate of Rollers	Rotation of the Mandrel	Mesh outside the box	Mesh inside the box	Trigger remesh when change in equiv. plastic strain is greater than
1	Sim-1	30°	1.323 mm/s	3.5 rev/s	0.8 mm	0.5 mm	0.1
2	Sim-2	30°	1.323 mm/s	3.5 rev/s	0.8 mm	0.4 mm	0.1
3	Sim-3	30°	1.323 mm/s	3.5 rev/s	0.8 mm	0.3 mm	0.1

Table 3.1 Parameters for the mesh size study experiments

For the modelling all the inputs were taken from Hayama's experiments. Some unit changes were applied as shown below:

$$N = 210\frac{rev}{\min} * \frac{\min}{60\sec} \qquad v = 0.378\frac{mm}{rev} * \frac{3.5rev}{1\sec}$$

$$N = 3.5\frac{rev}{\sec} \qquad v = 1.323\frac{mm}{\sec}$$

For these 3 models, remeshing boxes are used. Boxes are placed around workpiece and are stationary; there is no translational or rotational motion. General overview of the rollers, mandrel and tube can be seen in Figure 3.3.

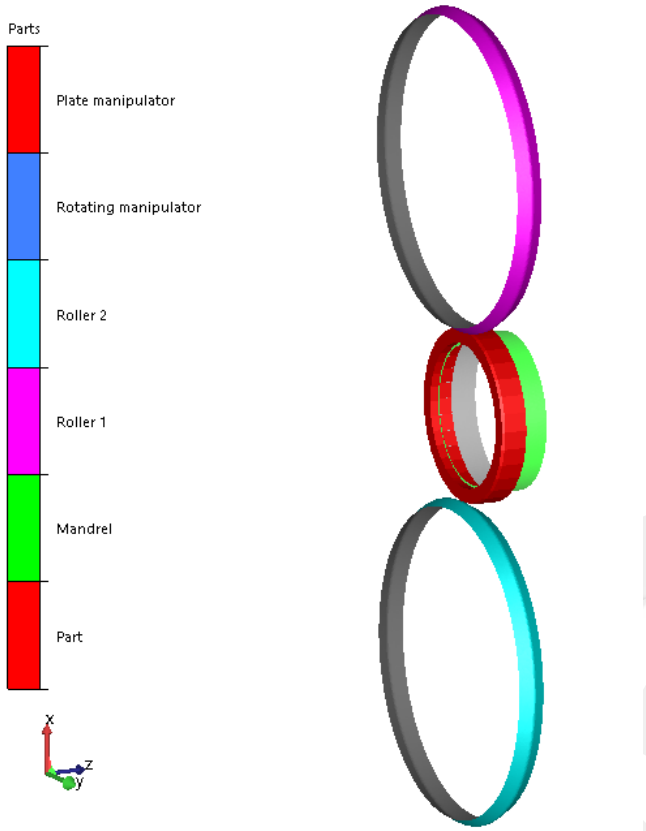

Figure 3.3 3D tube spinning setup

For the tube meshing, structured ring mesh model was used. The critical contact areas have more elements than the other sections. In this thesis, he same structured ring model was always used as shown below;

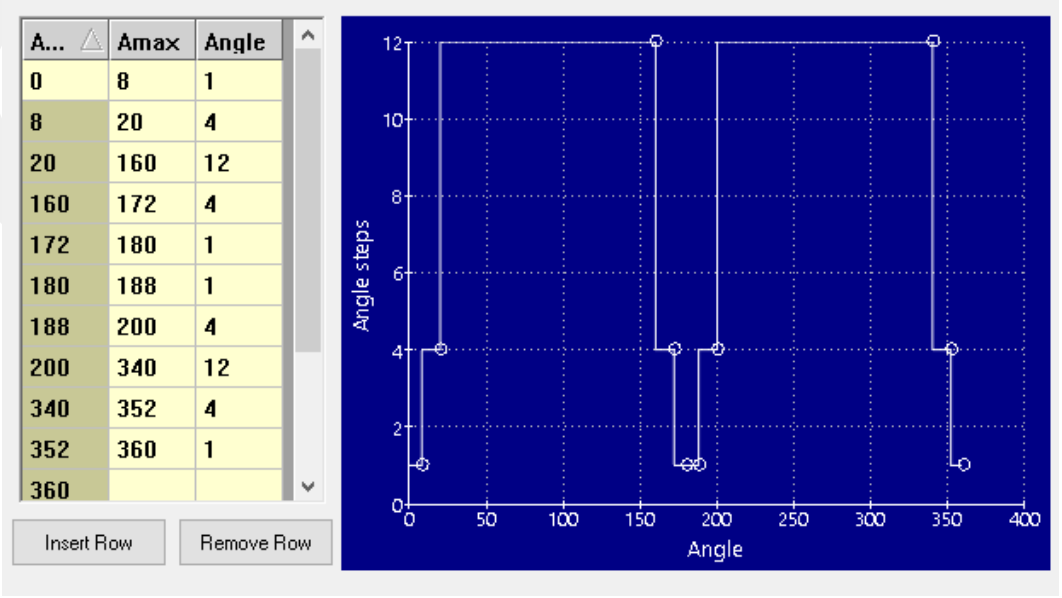

Figure 3.4 Structured ring mesh parameters

For the contact areas between workpiece and roller, 1^0 angled sections are used in order to get a good estimate of the surface contact. This 1^0 angled portions have to involve ellipsoid contact zone of the roller. By using structured ring mesh model, number of elements of the work piece decreases significantly. An overview of the structured ring mesh is shown below:

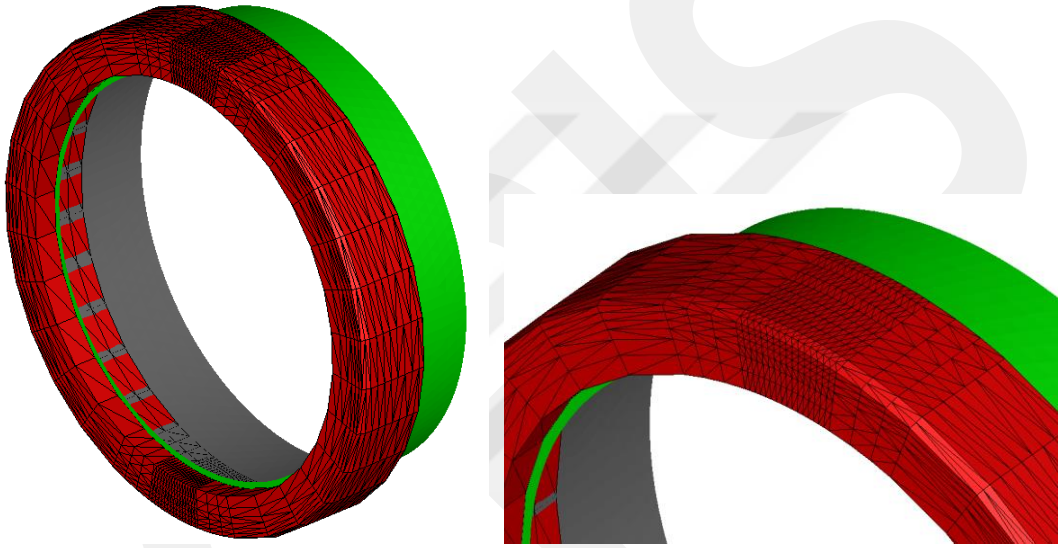

Figure 3.5 Structured ring mesh

Cylindrical remeshing box is used for these 3 analysis. They were placed around the tube and they have the same center axis with the work piece. The diameter of the remeshing box contains the deformation zone that stays under the rollers. Moreover, it has to contain wave in front of the rollers. The inner and outer diameter of the box are 22 mm and 19 mm. The sample of the remeshing box is shown at Figure 3.6.

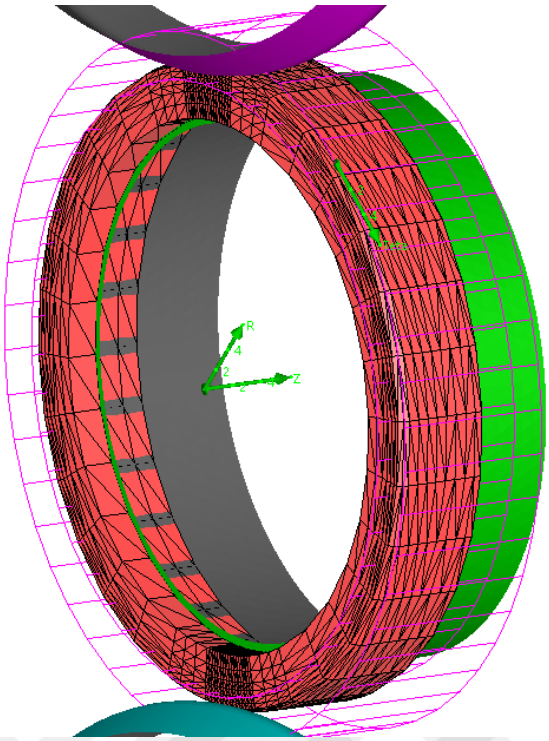

Figure 3.6 Remeshing box around the workpiece

Remeshing box's outer diameter is 2 mm over than the undeformed tube's outer diameter to include the material that piles up in front of the roller.

3.3.1.1 Force vs Mesh Sizes Comparison with Full Length Remeshing

From 2D analysis, it is known that after a certain point radial force is getting a constant value in the middle portion of the process. It can be also proven for 3D analysis. The figure that is shown below, belongs to radial force " F_r " on the upper roller.

For "Sim-1" analysis the mesh size inside the remeshing box is 0.5 mm and outside of the remeshing the mesh size is 0.8 mm. Length of the tube is 6mm and used rollers have 30^o the

Simulations have been solved with a computer that has Intel® Xenon® CPU E5-2640v3@ 2.60 GHz and 8 physical cores (16 logical processors) with a computational time of about 4.5 hours.

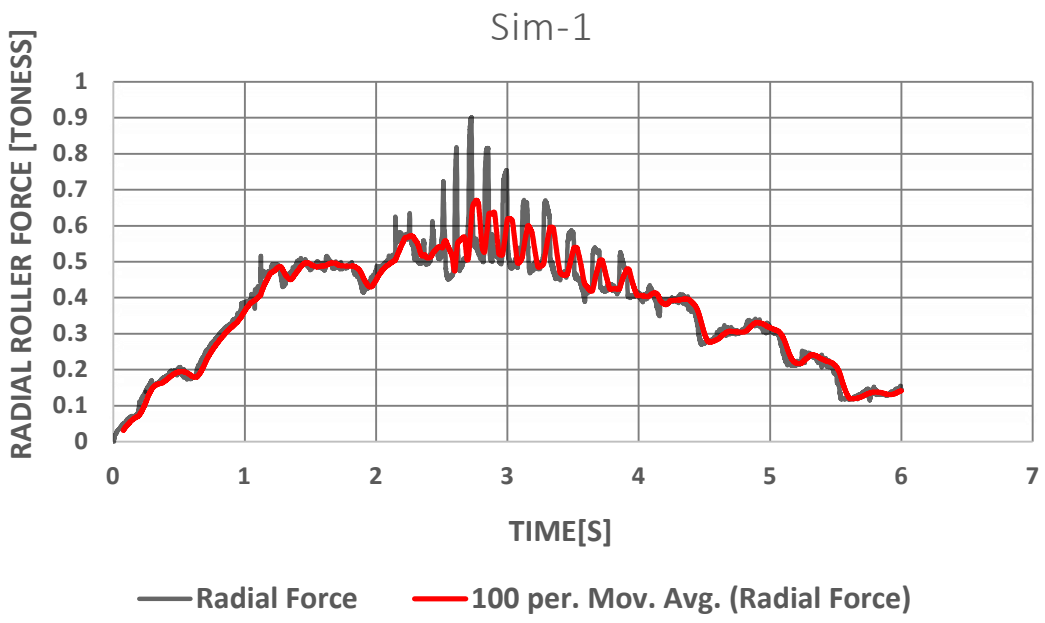

Figure 3.7 Radial force on roller in Sim-1

The force varies between 0.5 and 0.65 tones. The main reason for the force fluctuation is the continuously changing contact condition at the roller-tube interface, along with element size used in the mesh.

It can be seen that; from 2 seconds up to about 3.5 seconds; the radial force is getting a constant value the force and the process seem to be reaching a steady state condition. Therefore analyzing the process only up to the steady state point should be enough to obtain an estimate of the forming (roller) force.

The second simulation is “Sim-2”. Again the same type and same size of cylindrical remeshing box is used. However, this time the mesh size inside the remeshing box is set as 0.4 mm, and outside mesh dimension is again 0.8mm. Tube length and roller type have not been changed. Simulation is again performed on 16 logical processors and it has a computational time about 8 hours. The radial force, “R_r” on the upper side roller is shown below;

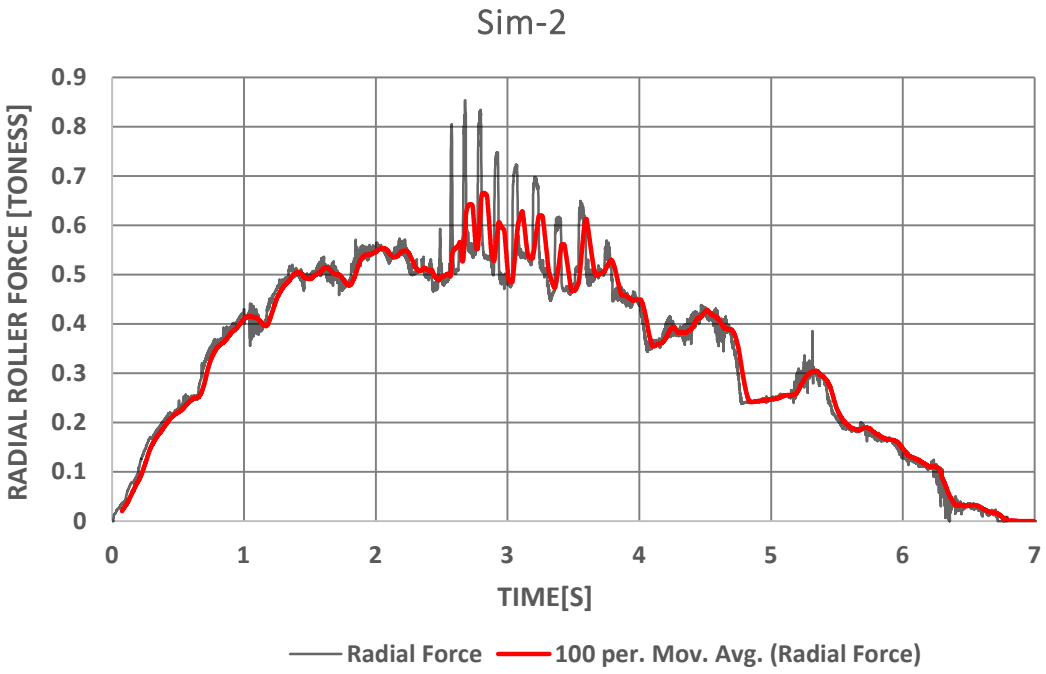

Figure 3.8 Radial force on roller in exp-2

The raw data (black line) fluctuates again, but when it is compared with the "Sim-1" simulation it has less noise and the lines' lengths between picking upper and lower points are less than before. This situation is related with the mesh size of the tubular blank. On the other hand, again F_r force is about 0.5 -0.65 tones on the roller, however the smoothed graph values are closer to 0.5 tones.

The third simulation was named as "Sim-3". The same size remeshing box that is cylindrical type around the workpiece is used. For this analysis, the mesh inside the remeshing box is set to 0.3 mm. Tube lengths and roller sizes are the same with other two simulations. Simulation is solved with 16 logical proessors and computational time takes about 16 hours. When the radial force vs time graph is examined, the peak values decrease when compared with other mesh sizes that are 0.5 mm and 0.4 mm. Moreover for steady state condition of F_r, the value is very close to 0.5 tones as in Hayama [4]. When all the analyses are examined, after a certain point tube spinning process get a steady state condition.

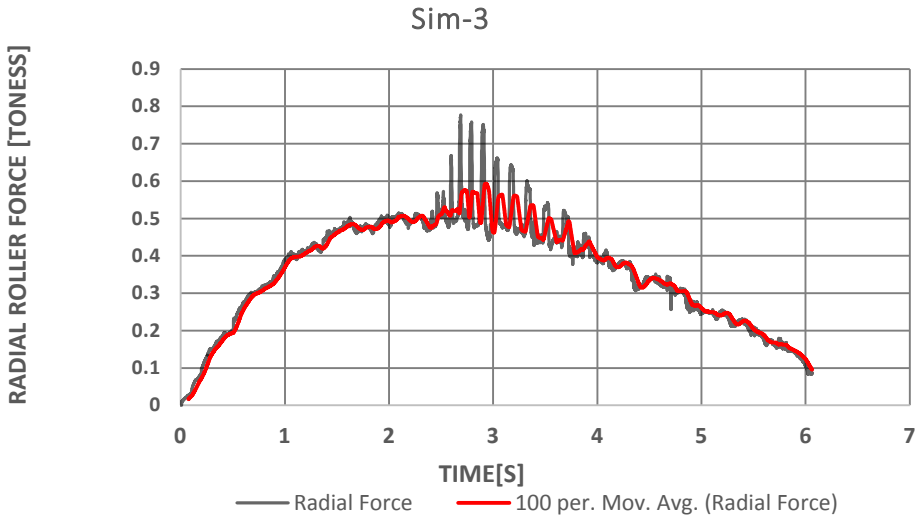

Figure 3.9 Radial force on roller in exp-3

For these analysis certain point is about 2 seconds. After 2 second, F_r is getting a value about 0.5 tones. Mandrel has a radius at the beginning to have a smooth contact with tube. Thickness of the tube is 2mm and 1 mm radius is at the beginning of the mandrel. After roller is passing mandrel's fillet edge, radial force "F_r" on the roller is getting a constant value and process starts to behave in steady state condition. In Hayama's experiment, radial force for the same situation is about 0.5 tones for 30° angled roller and 1.323 mm/sec feeding rate and 0.2 thickness reduction ratio, that graphic is shown below:

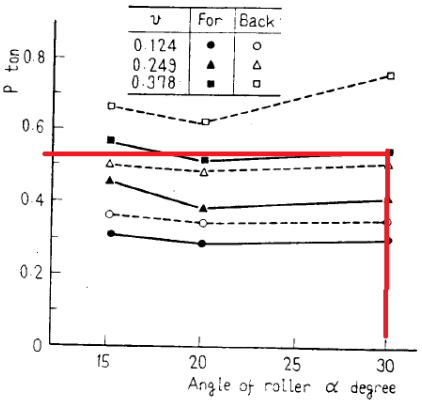

Fig. 16 Relationship between resultant force P and angle of roller (R_δ= 0.2)

Figure 3.10 Total force vs roller angle graphic [4]

While analyzing the simulation, 3 groups can be defined according to force situation. These are beginning period, middle period and finishing period. Periods can be divided according to the force values vs time intervals that are increasing, getting constant and

decreasing situations. Therefore, for other graphics, the special time will be 3rd second because it is the middle point of the analysis and middle point for the constant force. For all virtual experimental results, the outcomes look nearly the same. When radial force vs time graphics of roller are examined, they have the same behavior as shown in the below;

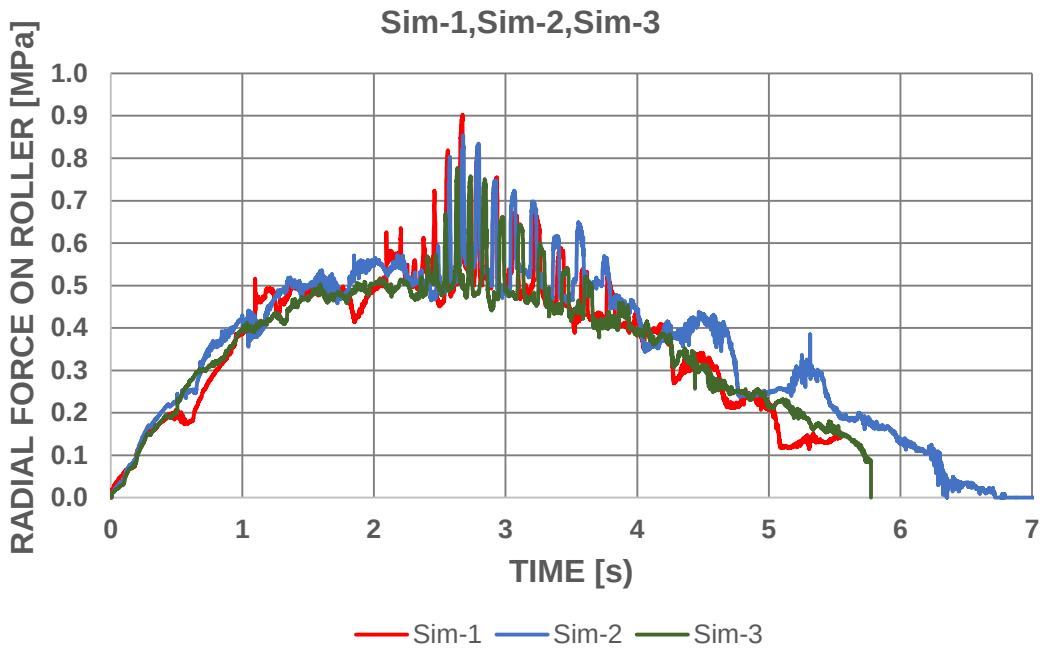

Figure 3.11 Radial forces vs time graphic for Sim1, 2, 3

As shown in the above averaged maximum radial force is about 0.5-0.6 tones. It says that with a course mesh, nearly correct radial force values can be calculated. That is important because mesh size directly affects the computational time. Therefore 0.5 mm mesh size can be accepted as the ideal size.

3.3.1.2 Strain Rate vs Mesh Size Comparison for Full Length Remeshing

For all analysis, strain rates distributions are examined. Strain rate gives information about the instantaneously deformation during process. When tube spinning process is performed, the affected zones are just under the rollers instantaneously. Affected zone means that currently plastic deformation zones and it can be defined from strain rate distribution. The most important point is that strain rate can penetrate up to the bottom surface of the work piece. Because of this, tube's length can elongate with the same direction of feeding. However, always the maximum deformation is on the upper

surface of the tube. Therefore, forming velocity of the upper surface more than the lower surface and resulting of this nonhomogeneous deformation occurs end of the process. For the analysis Sim-1, 2 and 3, strain rates can be examined. In the figures below, strain rates are shown for the analyses Sim1, 2 and 3;

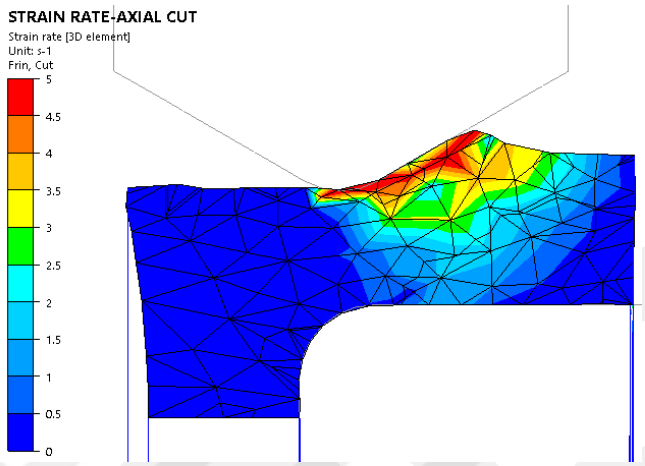

Figure 3.12 Strain Rate Distribution for Sim-1

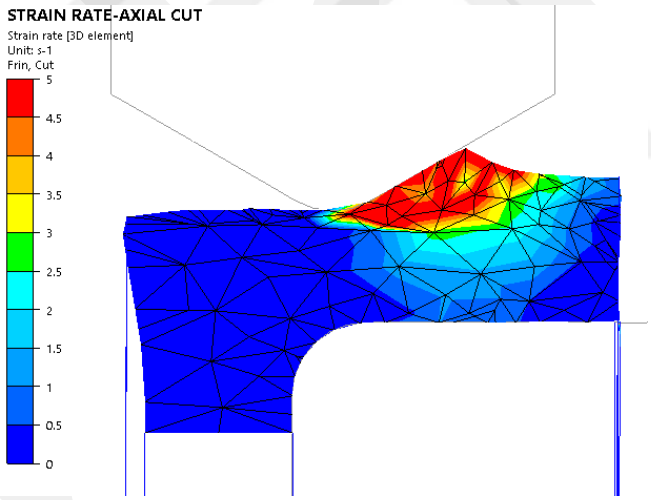

Figure 3.13 Strain Rate Distribution for Sim-2

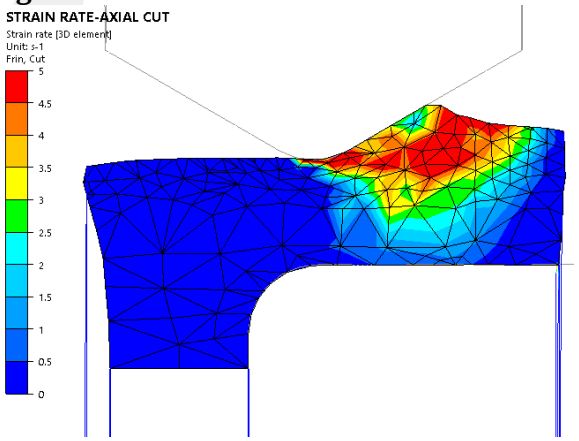

Figure 3.14 Strain Rate Distribution for Sim-3

For strain rate visuals, same size colored legends are used for the same instant in order to compare distributions vs mesh sizes. It is obvious that there is no significant differences along different mesh sizes, their distributions are similar. The common results is the decreasing strain rate as going from outer to inner surface of the tube. Because force is directly applied from upper surface and it is transmitted from upper surface to inner surface, as passing through the thickness, material resists and deformation rate is decreasing.

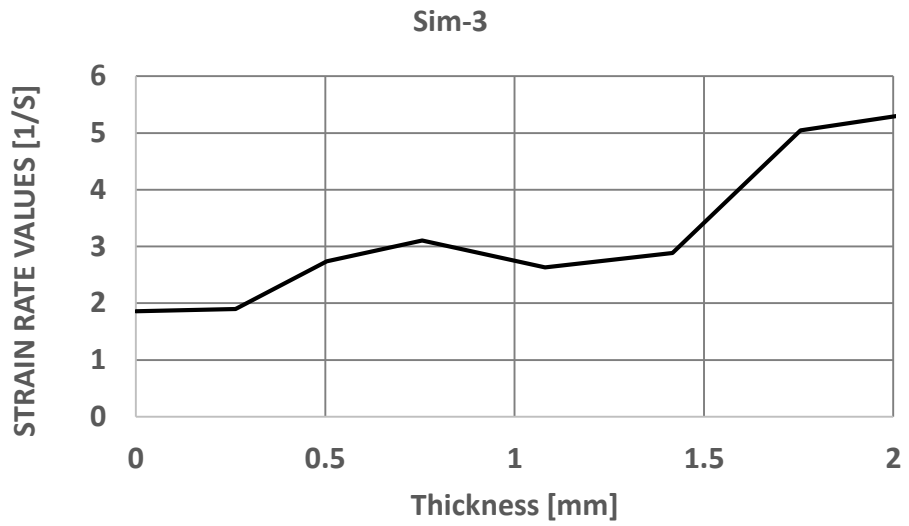

Figure 3.15 Strain rate distribution from inner to outer surface of tube

In Figure 3.15, strain rate distribution is shown for Sim-3. It is obvious that strain rate is maximum at tube's outer surface and minimum at tube's inner surface. However at tube's inner surface it is not zero, it exists. This proves that deformation can penetrate up to inner surface and therefore tubes length is elongating during tube spinning process. If it was not able to reach up to the inner surface, at beginning of the process, non-homogeneous plastic deformation would happen. Furthermore, discontinuity or cracks would be happen. On the other hand, process is axisymmetric, at this instant deformation, strain rate distribution and any other process results are same for the second roller. Therefore, in this study although two rollers are used, for figures just one roller is shown. For instance, for Sim-3 virtual experiment, strain rate distribution under second roller is shown in the Figure 3.18.

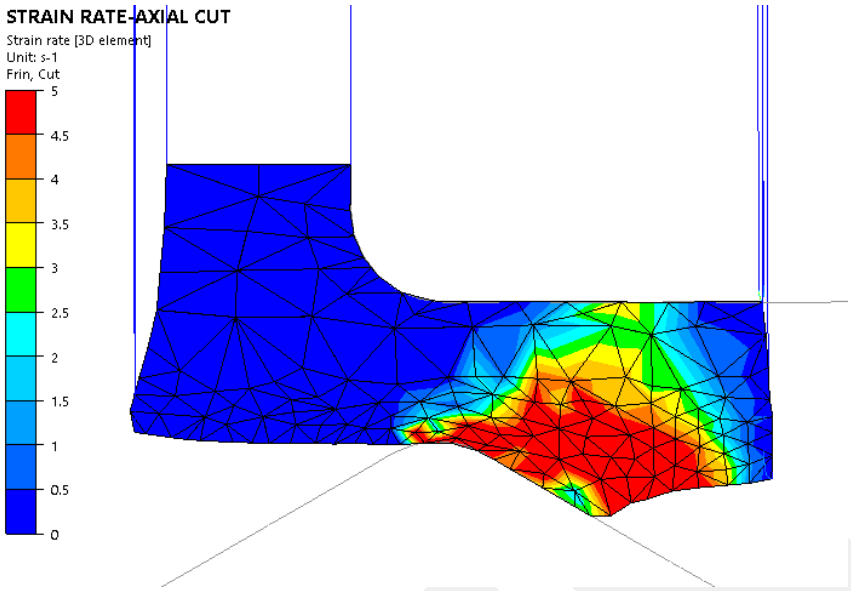

Figure 3.16 Strain rate distribution under second roller for Sim-3

3.3.1.3 Von Mises vs Mesh Size Comparison for Full Length Remeshing

Von Mises stress is examined for different mesh sizes. When the strain rate and von Mises stress distributions are compared for all mesh sizes, there is an available conflicting that is currently deforming zones. From strain rate, the plastic deformation localizes under the roller for the same instant. However, von Mises stress shows that plastic deformation does not ended for the just behind of the roller. This situation can be related with the mesh size of the part. However it is rational that, when looked to the von Mises stress distribution it is also localized deformation zone under the roller.

For Sim-1, Sim-2 and Sim-3 von Mises stress values are shown for the same instant. Same legend is used and max stress value set to 850 MPa and min stress value is set to 0 MPa. There is no big differences between three different mesh sizes. But in Sim-3 which has the finniest mesh, von Mises values in front of the roller are less than the other two virtual experiment. When the strain rate and von Mises stress distribution are compared, von Mises stress distribution shows the elastic and plastic deformation at the same time, because of this plastic deforming zone looks like higher than the strain rate's shown. Therefore, for the instantaneous deformation zones should be viewed from the strain rate distribution.

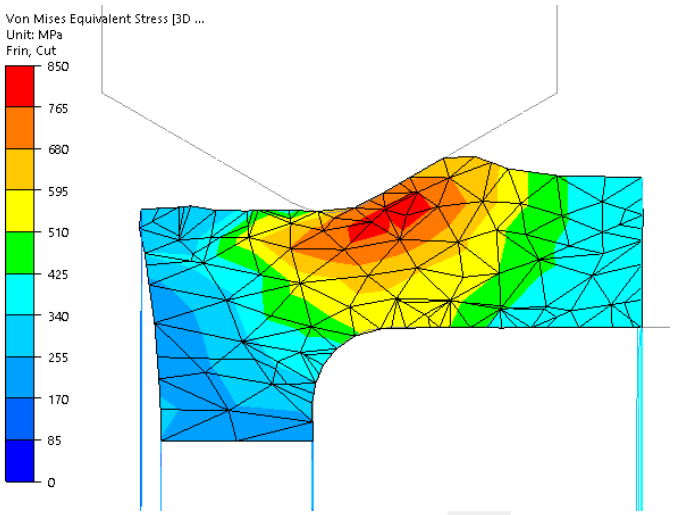

Figure 3.17 Von Mises stress for Sim-1

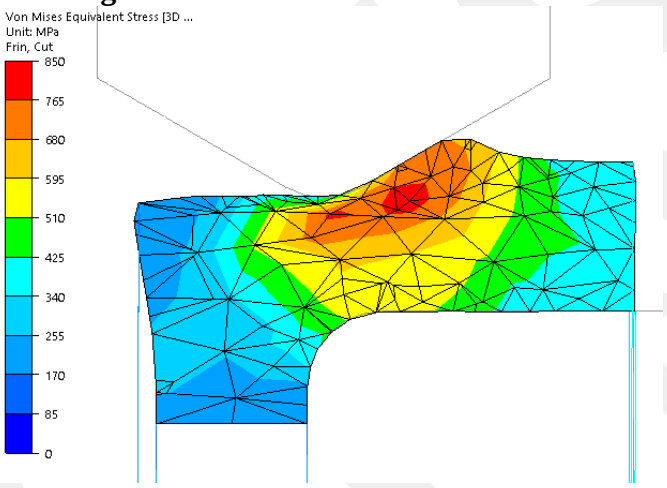

Figure 3.18 Von Mises stress for Sim-2

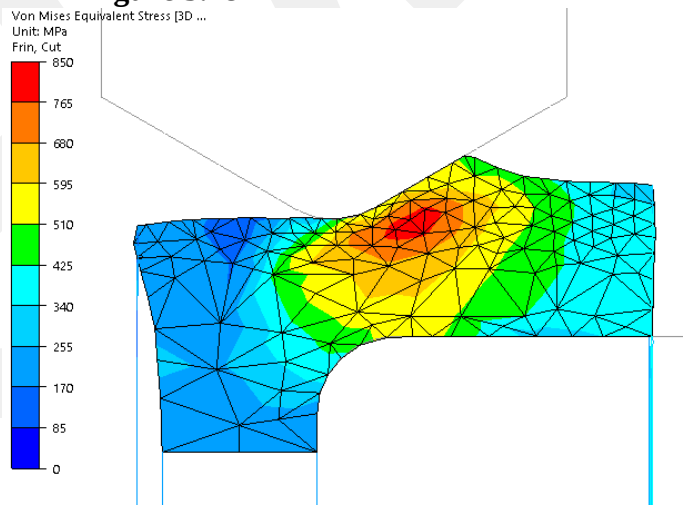

Figure 3.19 Von Mises stress for Sim-3

3.3.1.4 Mesh Size vs Computational Time Comparison for Full Length Remeshing

Overall, the number of elements at 3rd, fine remeshing sizes and total computational times are shown in the table below;

Table 3.2 Simulation elements number vs computational time

#	Simulation Name	Default Mesh Size	Remeshing Mesh Size	Number of Elements	Computational Time
1	Sim-1	0.8	0.5	29988	4 Hours 26 min
2	Sim-2	0.8	0.4	30396	8 Hours 16 min
3	Sim-3	0.8	0.3	53652	16 Hours 20 min

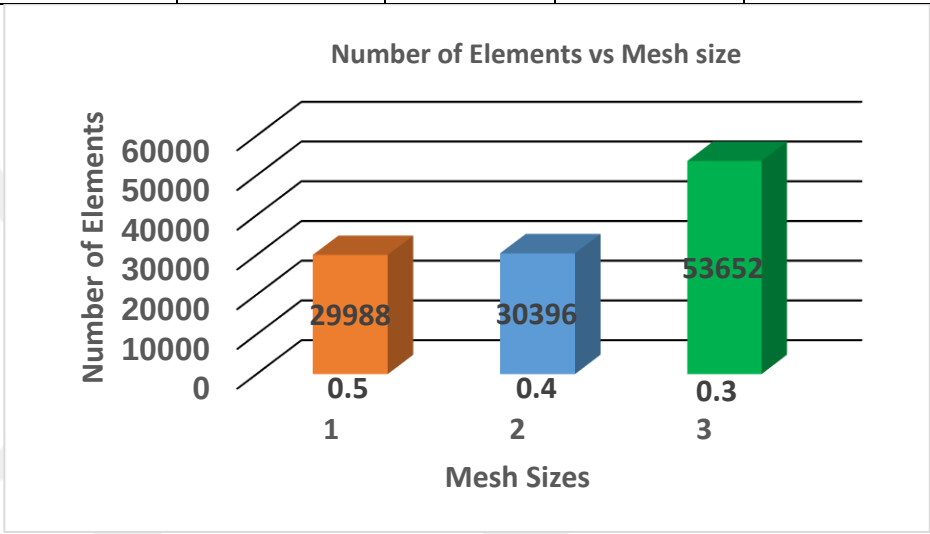

Figure 3.20 Number of elements vs mesh size

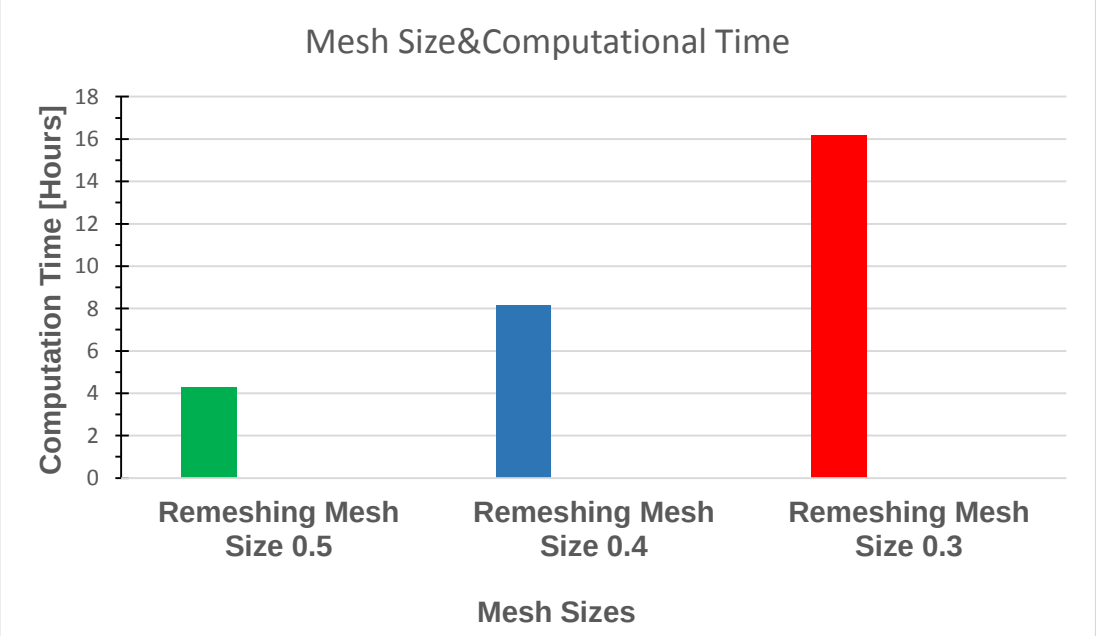

Figure 3.21 Computation time vs mesh size

When we analyze the graphs, the optimum parameters for calculation has been selected for next analysis. When numerical parameters that are for instance von Mises stress and strain rate are examined, all of the analysis have close results as numerical values and distribution. However, number of the elements in deformable tube directly effects the computational time. Therefore, in order to reduce the computational time for the full length of the tube spinning simulation, 0.5 mesh size is the best suitable mesh size.

3.3.2 Local Remeshing Box

Another different remeshing box method was applied to all of the models. Structured ring mesh is still applied on the tube with same angular partitions. Remeshing box is placed around upper or lower rollers and the shapes of the boxes are cylindrical. Center of the rollers and boxes' are concentric, moreover remeshing boxes are slave move with rollers. Therefore, they have rotational and translational movements. As the rollers move, remeshing boxes move with the same direction. By doing this, number of elements on the tube are decreased, so computational time can be reduced. Moreover, for the tube spinning process, current deformation zone is under roller. In this method deformation zone can be completely fine meshed and also this situation directly affects the result of the calculations. Used remeshing box method is shown below;

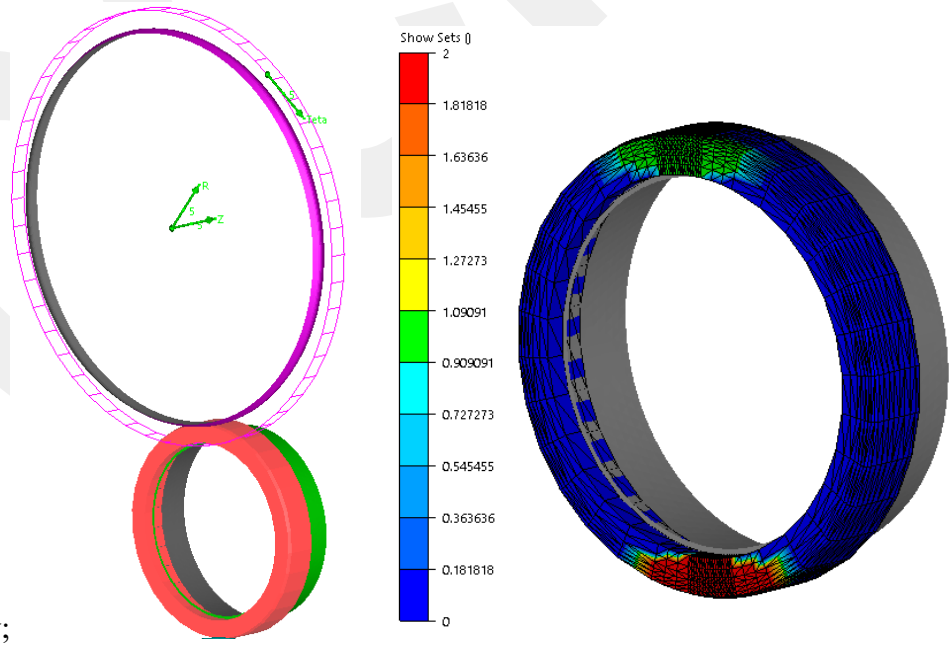

Figure 3.22 Deformation Zone Remeshing Box setup

For tube spinning simulations 2 rollers were used, one roller is shown on upper side, other roller also has the same remeshing box. In Figure 3.22 right side view shows where the remeshing boxes applied fine mesh on the tube, green is upper fine mesh zone, red is below fine mesh zone and both of them have the same volume. Cross sectioned view is shown in Figure 3.23.

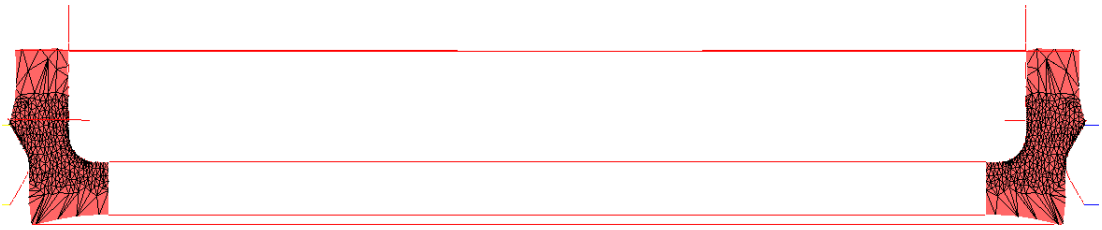

Figure 3.23 Local remeshing box cross sectioned view

In order to compare and decide which mesh size is enough to get an accurate data from the analysis, 0.5, 0.4, 0.3 and 0.2 mesh sizes were used during virtual experiments for this type of remeshing box. Moreover, to compare and decide which remeshing box model is the best, same rollers, mandrel and structured ring meshed tube were used. During the analysis, remeshing on deformation was closed but remeshing on deformation was applied every single 1000 increments.

#	Simulation Name	Roller Angle	Feeding Rate of Rollers	Rotation of the Mandrel	Mesh in out of Box	Mesh in remeshing Box	Remeshing with Period
1	Sim-4	30°	1.323 mm/s	3.5 rev/s	1 mm	0.5 mm	1000
2	Sim-5	30°	1.323 mm/s	3.5 rev/s	1 mm	0.4 mm	1000
3	Sim-6	30°	1.323 mm/s	3.5 rev/s	1 mm	0.3 mm	1000
4	Sim-7	30°	1.323 mm/s	3.5 rev/s	1 mm	0.2 mm	1000

Table 3.3 Simulation parameters used for the local remeshing box

3.3.2.1 Force Mesh Size Comparison for Local Remeshing Box

First examination is about time vs Radial force on the roller, "F_r". For all models upper side and bottom side of the tube have the same fine remeshing distribution for inside of the local remeshing box. Therefore, more smooth force vs time curves can be observed during the deformation. For all simulation F_r vs time graphics are examined.

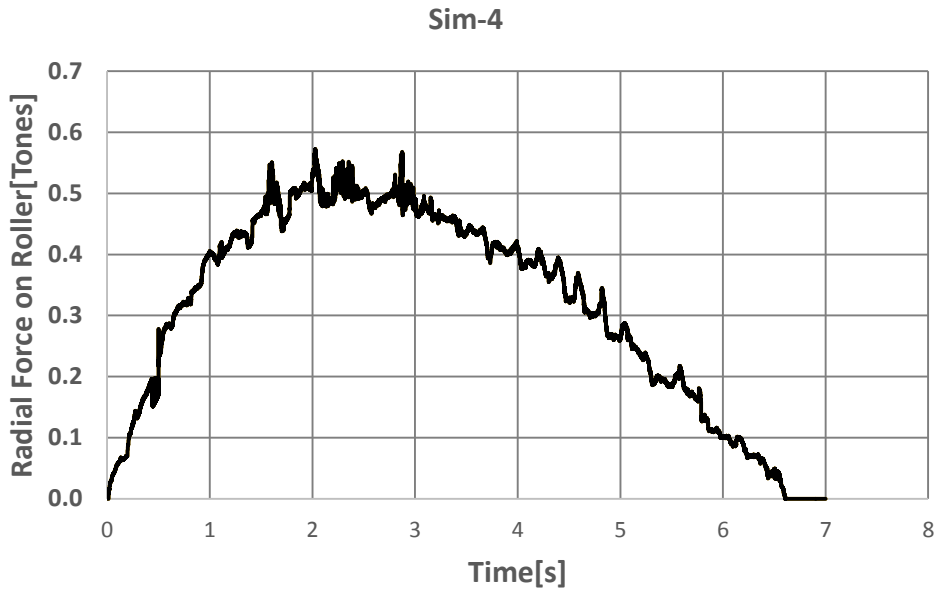

Figure 3.24 Time vs radial force for Sim-4

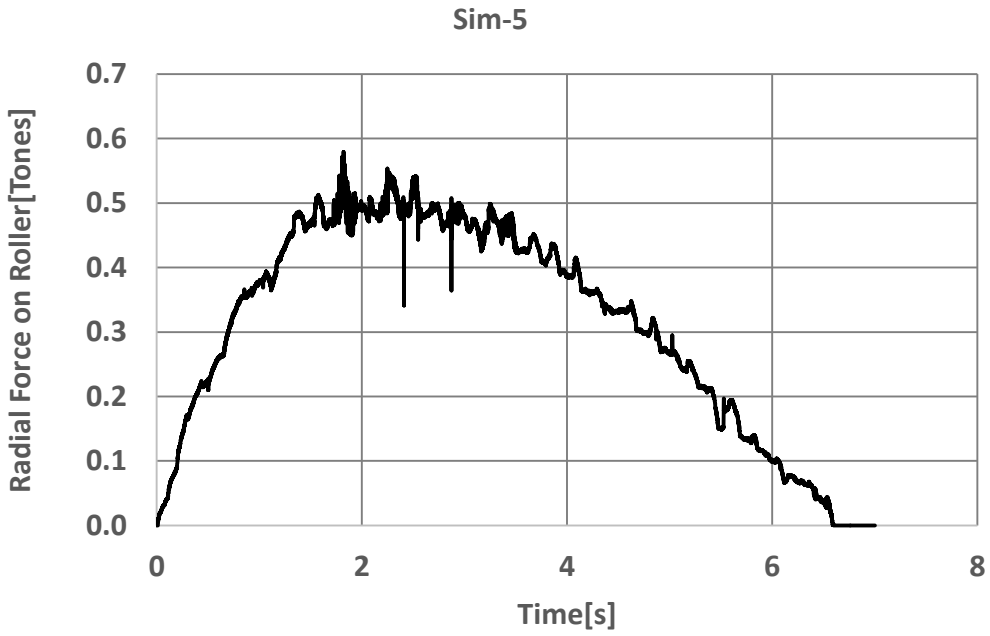

Figure 3.25 Time vs radial force for Sim-5

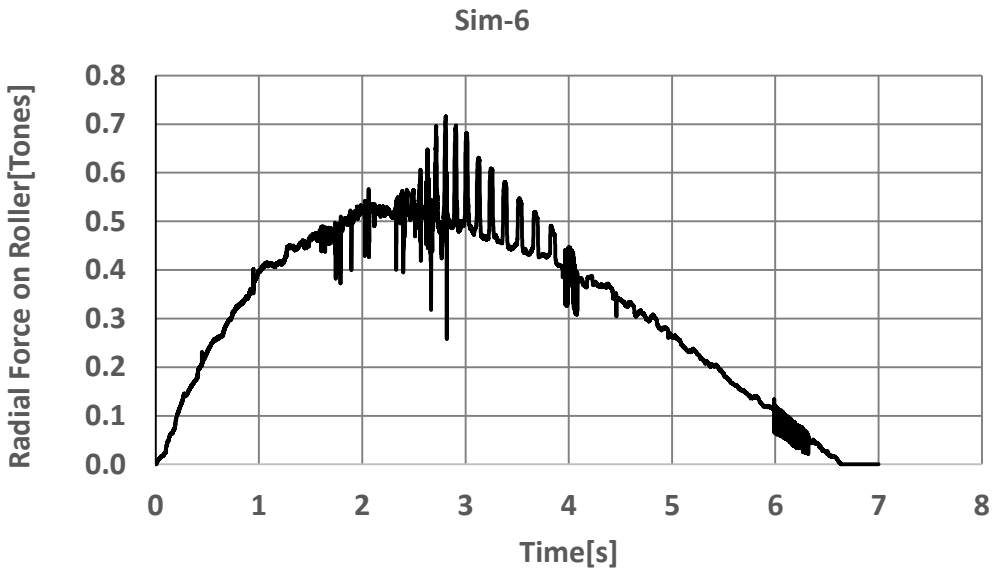

Figure 3.26 Time vs radial force for Sim-6

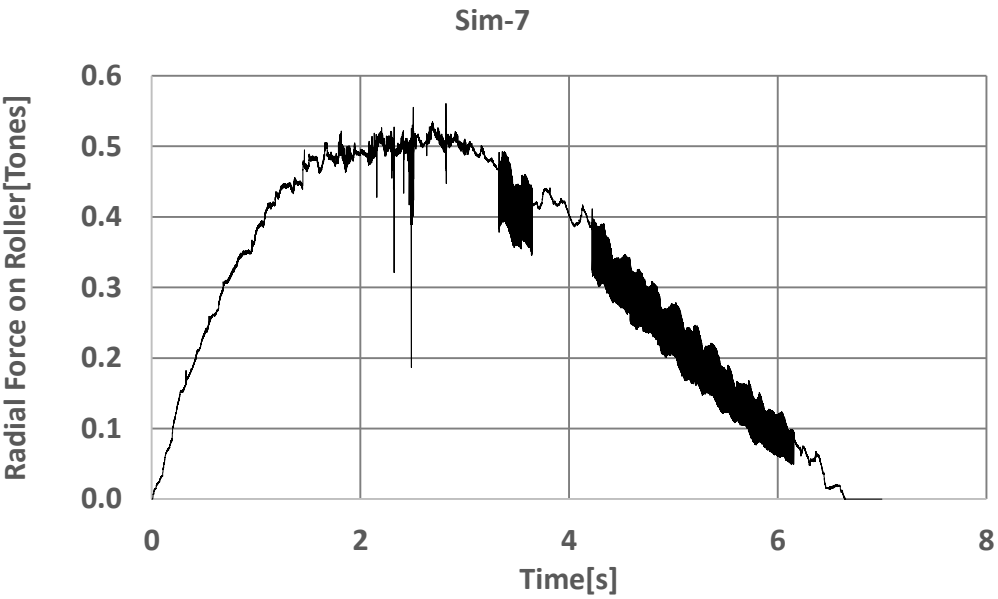

Figure 3.27 Time vs radial force for Sim-7

First of all, for all analysis it is obvious that after a certain point tube spinning process gets the steady state condition and radial force that acts on the roller is getting a constant value that is about 0.5 tones. Therefore, this situation proves that there is no need to analyze all length of the tube if the radial force is desired to be calculated.

Moreover, in order to reduce the computational time, for the force calculation, rough mesh can be used with remeshing boxes that are placed around the rollers.

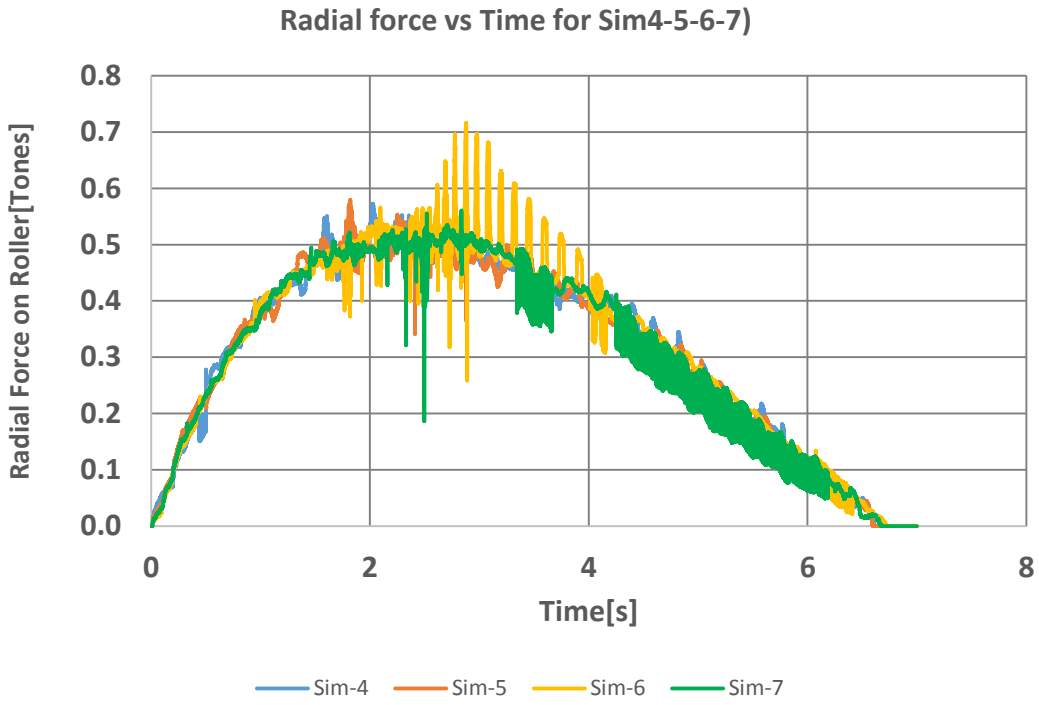

Figure 3.28 Time vs radial force for Sim-4-5-6-7

As shown in the table above maximum radial forces are nearly same for all four virtual experiments and its value is about 0.5 – 0.6 tones. However it is obvious that Sim-7 analysis has the max fine mesh which is 0.2 mm but it has the maximum noise because of during process there are lots of contact nodes at the surface between roller surface and tube's upper surface, as roller and tube contact in and out, peak points amount is increasing.

3.3.2.2 Strain Rate vs Mesh Size Comparison for Local Remeshing

For the strain rates, the mesh size important to observe instantaneous effected zone by the deformation. The main point is; deformation should reach up to bottom side of the tube. For all model, radial force is getting a constant value after 2 seconds. 3rd second is accepted for middle portion of the analyses and max radial force occurs at 3rd second. Therefore, for the strain rate distributions are examined for 3rd second. Same size legend is used for strain rate distributions.

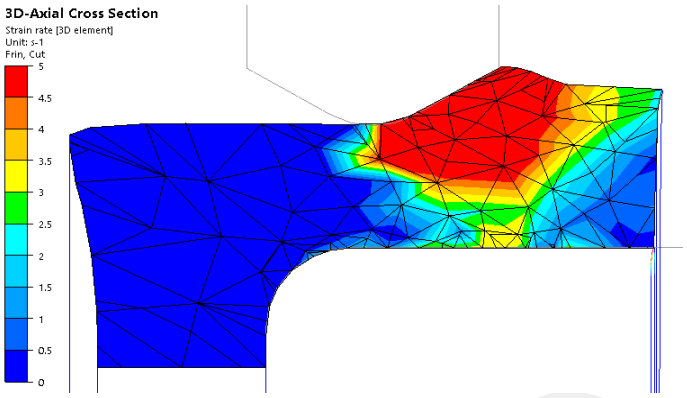

Figure 3.29 Strain rate distributions for Sim-4

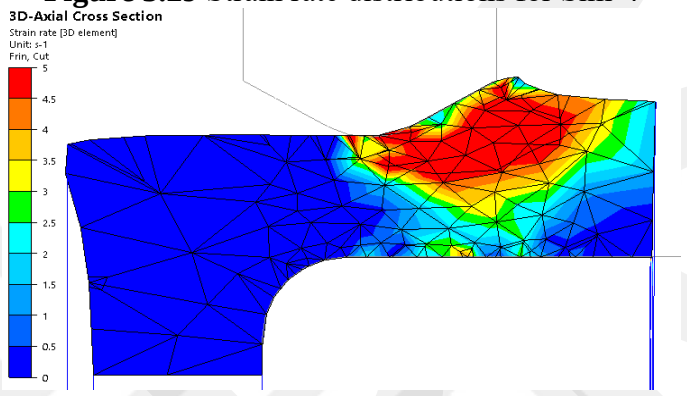

Figure 3.30 Strain rate distributions for Sim-5

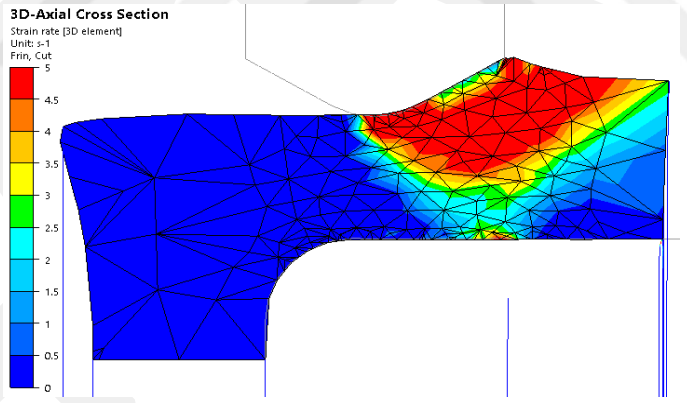

Figure 3.31 Strain rate distributions for Sim-6

When four different mesh size strain rate distributions are examined, for the mesh sizes 0.5 mm, 0.4 mm and 0.3 mm have nearly the same strain rate distribution. However, 0.2 mm mesh size's strain rate distribution looks like different from others. In Sim-7, deforming rate is more than the Sim-4-5-6 at the inner surface of the tube. Therefore, mesh size of the three dimensional tube spinning process directly affects the strain rate distributions along a thickness. However as selecting the finer mesh size, analysis's

computation time will elongates. Therefore, course mesh strain rate can give an approach about the process mechanism. On the other hand, strain rate vs thickness distribution is shown in the Figure 3.32 for Sim 7

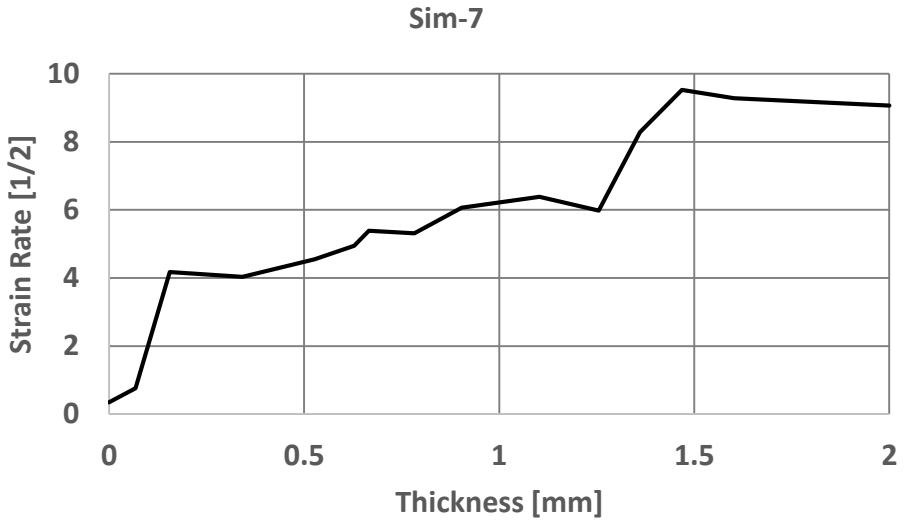

Figure 3.32 Strain rate distribution from inner to outer surface of tube

3.3.2.3 Von Mises vs Mesh Size Comparison for Local Remeshing

Von Mises stress includes not only elastic stress but also plastic stress. For the simulations von Mises gives information about plastic deforming zones. But it includes elastic stresses. If the von Mises stress is more than the yield stress of the material, that zones can be accepted as plastic deformation exists. For the tube spinning process, deformation zone occurs according to roller size and roller numbers. If mesh size decreases, von Mises distribution will not change as shown in the figures.

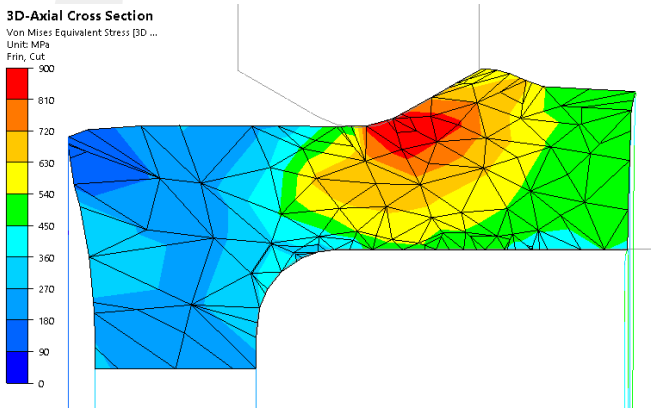

Figure 3.33 Von Mises stress distribution for Sim-4

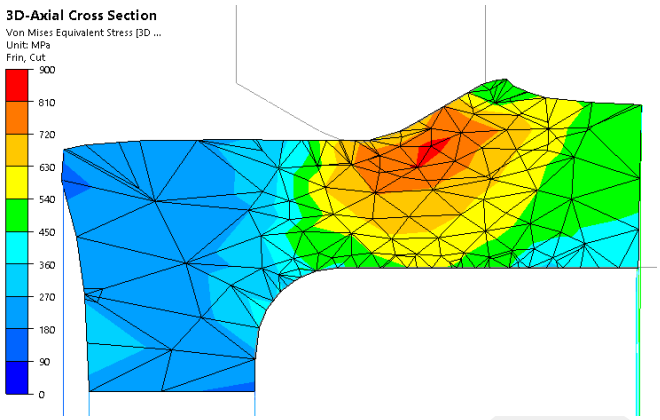

Figure3.34 Von Mises stress distribution for Sim-5

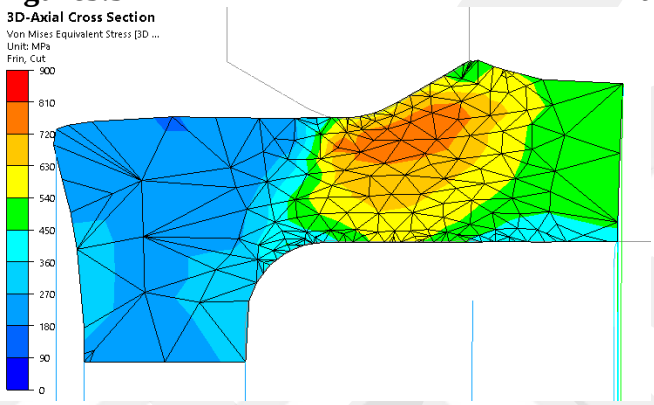

Figure3.35 Von Mises stress distribution for Sim-6

3.3.2.4 Mesh Size-Computational Time Comparison for Local Remeshing

Three dimensional tube spinning finite element analysis takes more time than other forming operations' analysis. The used element number is decisive for the computational time. Used element number affects the calculation time, because in tube spinning process all the meshes have the rotational and translational motion or rotation motion. When graphics are examined again the fastest analysis has the 0.5mm mesh size.

Table 3.4 Elements number vs computational time for local remeshing box

#	Default Mesh Size	Remeshing Mesh Size	Number of Elements	Computational Time
Sim-4	0.8	0.5	30600	7 Hours 39 min
Sim-5	0.8	0.4	38352	14 Hours 43 min
Sim-6	0.8	0.3	58344	24 Hours 43 min
Sim-7	0.8	0.2	117708	70 Hours 0 min

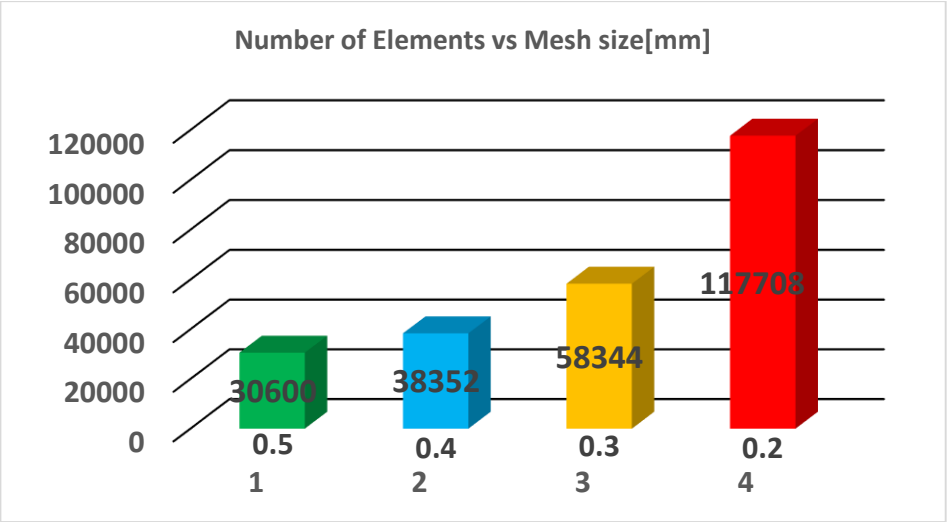

Figure 3.36 Number of elements vs mesh size

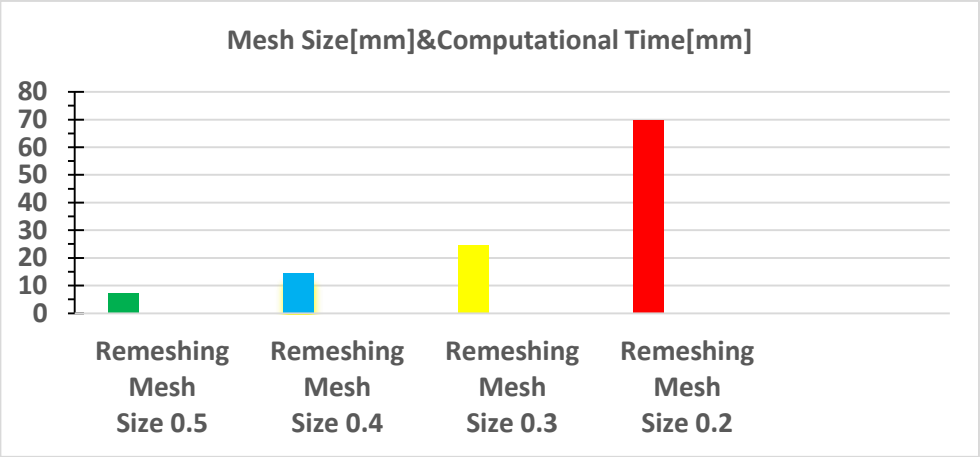

Figure 3.37 Computation time vs mesh size

3.4 Wave Shape Comparison

From three dimensional analysis, wave formation can be observed. Hayama [4] drawn graphs about behavior of wave in front of the roller .They were categorized according to feeding velocities, roller angles and reduction levels as shown in Figure 3.39. Sim-1 can be compared with 6th experiments in the figure. In the three dimensional model, same wave can be observed. Shape of the wave is directly related with the reduction level and rollers angle, as they increase, wave's volume and angle will increase;

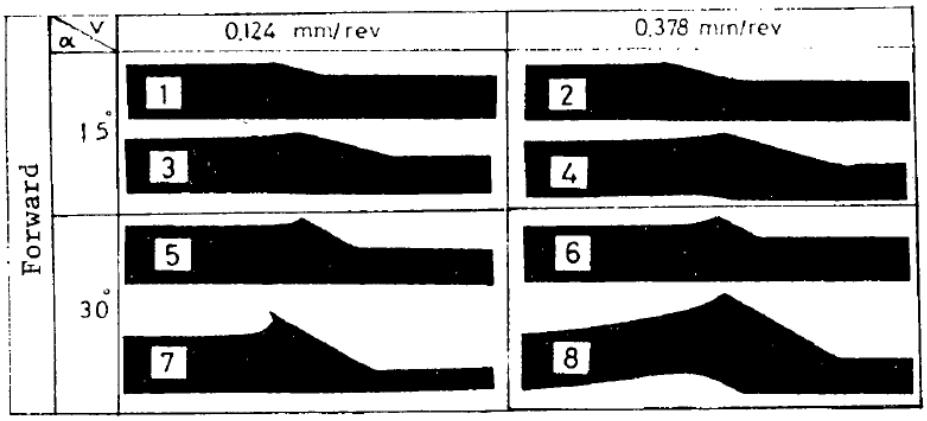

Fig. 6(a) Shape of wave in forward tube spnning
R_o: (1) 0.20 (2) 0.25
(3) 0.39 (4) 0.34
(5) 0.34 (6) 0.21
(7) 0.57 (8) 0.37(unsteady)

Figure 3.38 Tube spinning wave formation, [4]

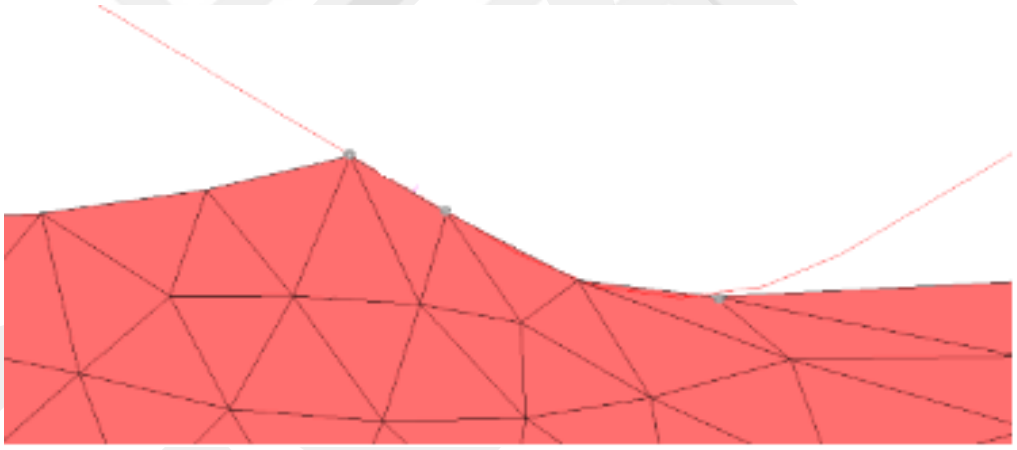

Figure 3.39 Tube spinning wave formation

Figure 3.38 and 3.39 have the same process parameters which are material, roller geometry and reduction ratio. In order to compare Hayama [4] and virtual experiments, these two views are superposed and they have the same wave formation as shown in the Figure 3.40;

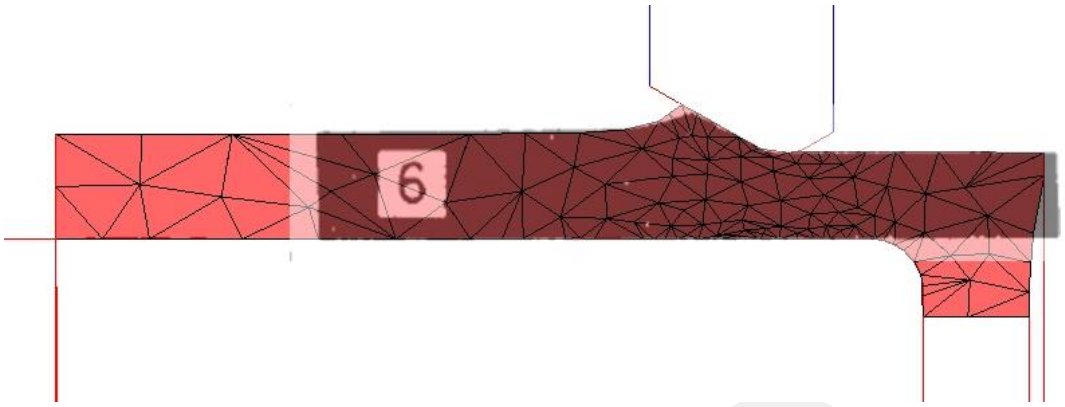

Figure 3.40 Wave comparison of virtual experiments and [4]

3.5 Conclusion of Three Dimensional Modelling

In this chapter seven different virtual experiments are mentioned. All analyses are examined according to their mechanical properties which are strain rate and von Mises stress values. Moreover, radial force on the rollers are compared. Two different remeshing box types are tried. And the result is that, analyses which have full length type remeshing box, are computed faster than the local remeshing box used analysis. On the other hand, different mesh sizes are tried. Mesh size directly affects the computation time. In the results, there is no significant differences. Therefore, 0.5 mm mesh size should be selected for modelling and analyzing of the tube spinning process.

3.6 Introduction to Mechanism

In this chapter, mechanical properties and flaring mechanism are explained. Only one analysis is used in order to explain mechanical properties and flaring mechanism. Just three dimensional model is used. Mesh size is selected as 0.5mm, in order to reduce to computational time. Because tube is modelled 18mm. The tube's length is increased because flaring mechanism cannot be observed in short length model.

3.7 Mechanism of the Tube Spinning Process

In tube spinning process, tubular blank is fitted on the rotational mandrel. Besides, like the workpiece and mandrel, forming rollers also have rotational motion around their

own axis. Forming rollers approach to the blank and plasticize the tubular blank. By this means, length of the rotational blank is increased along the axial direction and the wall thickness is reduced along the radial direction.

There are two main purpose of performing tube spinning process; one of them is reducing the thickness of the tube another is increasing the length of it. In order to make both of them, there is only one condition should be satisfied during the process. While deforming the material two contact area can be examined; contact area under rollers through the axial direction and the contact area through the circumferential direction. If the circumferential contact length more than the axial contact length; forming will performed along the axial direction because metal flow come across less resistance along the axial direction and tube's length can elongate along axial direction. Because of this deformation mechanism process can be likened to the simple extrusion process. If the deformation mechanism has the reverse situation; circumferential contact area less or close to the axial contact area, deformed material flows along circumferential direction and tube will not elongate. However, there will be elongation in circumferential direction as well, in other words, tube will start growing in diameter. Since this is undesirable in this process, the process is stopped.

3.8 Final Length Prediction

Tube spinning process's dimensional variables are shown in figure below. L_0 is the blank length, S_0 starting thickness, S_1 final wall thickness, d_1 internal diameter of blank and L_1 is the final length of the workpiece. When volume constancy assumption is made, workpiece volume will be constant after deformation process. Therefore, the formula which is seen below, can be used in order to predict the final length of the tube. Final length depends on the initial length, initial thickness, final thickness and internal diameter of the tube.

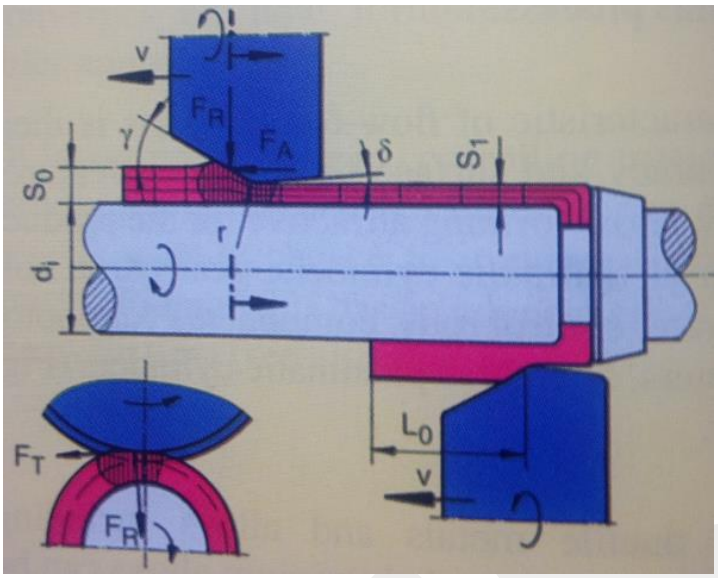

Figure 3.41 Tube spinning dimensional length parameters' labeling [14]

$$L_1 = \frac{L_0 * S_0 * (d_i + S_0)}{S_1 * (d_i + S_1)}$$

At the end of the process, end of the tube will be deformed none uniformly. Therefore, after process is finished, a fair amount blank has to be cut from end of the tube. Besides, formula only gives an approximate idea about the final length of the tube. In process mechanism chapter, only a virtual experiment was selected. All examinations and commends had been done on it and selected virtual experiment's all process data is shown at Table 3.5.

Table 3.5 Used modelling parameters

Parameters	Symbol and units	Values
Diameter of mandrel	d (mm)	36
Diameter of roller	D_R(mm)	74
Angle of roller	α = β (deg)	15°
Number of roller	n_o	2
Number of rotation of mandrel	N (rpm)	210
Feed of roller	v (mm/rev)	0,378
Thickness of tubewall	t_o	2
Yield point of tube	σ (Mpa)	225,63 Mpa
Degree of thinning	R_o	0.2

$$L_1 = \frac{L_0 * S_0 * (d_i + S_0)}{S_1 * (d_i + S_1)} \Rightarrow L_1 = \frac{18 * 2 * (36 + 2)}{1.6 * (36 + 1.6)} \Rightarrow L_1 = 22.73mm$$

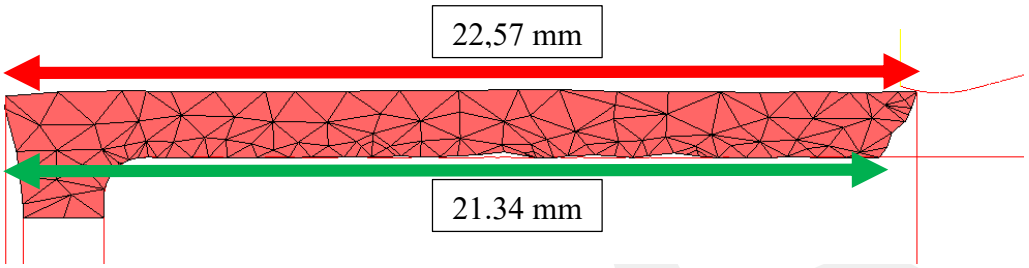

Figure 3.42 Tube length after deformation

After the deformation, length of the tube will elongate from 18 mm to 22.73 mm analytically. From the virtual experiments that has been performed by finite element method; the perpendicular distance between end of the tube edge and beginning edge is about 22.57 mm. This situation proves that final tube length of tube spun product can be predicted from virtual experiment that is performed by finite element method with a ± 0.5 precision. At the end of the process, tube's final length can classified in two categories. One of them is final uniform tube length another is final maximum tube's length. Maximum tube length is 22.57 mm and maximum uniform tube length is 21.346 mm.

3.9 Strain Rate

In order to clarify the deformation mechanism of tube spinning process strain rate is examined from 2 different cutting plane. Roller moves along z direction and mandrel and tube rotate along positive z direction. Under these conditions, strain rate gives information about during tube spinning which areas are instantaneously deforming under roller. For axial and radial direction cutting plane strain rate's visual, the same legend size is used, also visual belongs to the same process time. When looked to the axial direction section of the deforming tube, the first result is deformation direction is related with the feeding direction of the roller, rollers are moving along to the z direction and deforming zone is formed in front of the tube or with another saying just right of the roller's tip radius. This situation explains the basics of the tube spinning which is the tube's length could be elongated via tube spinning process in direction of

the roller's feeding direction. Moreover this situation is also valid for radial directional cutting view. System rotates about positive Z direction and deformation does not take place at the origin, deformation is formed just right of the roller center or system origin. Because right region of the roller has the first initial contact that is defined according to the turning direction of the tube.

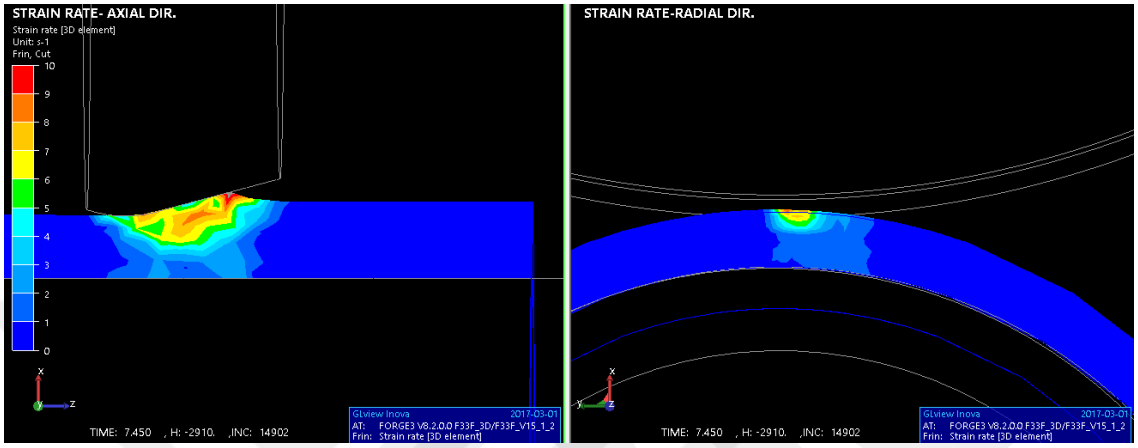

Figure 3.43: Strain rate axial and radial cross section

On the other hand, deformation localizes under a certain area. Strain rate shows the instantaneously deforming zones. For both axial and radial directional cutting sections, localized deforming zones can be seen in the Figure 3.43. From starting to the end of the tube spinning process deformation occurs and localizes just under and right region of the rollers.

The maximum deformation occurs at the contact zone between roller and deforming tube. Thickness reduction mechanism is performed at the top surface of the tube, therefore maximum displacement of material and deformation become at the top of the surface. From both view, maximum deformation can be seen. However the most important point is that during deformation process, the deformation can also penetrate up to the bottom surface of the tube. Because of this full penetration, tube's length can increase according to rolling direction homogeneously. If the penetration had not reached up the inner radius of deforming tube, tube's length cannot be elongated homogeneously and moreover may be deformation cracks could become because of non-homogeneous deformation distribution along radial (thickness) direction.

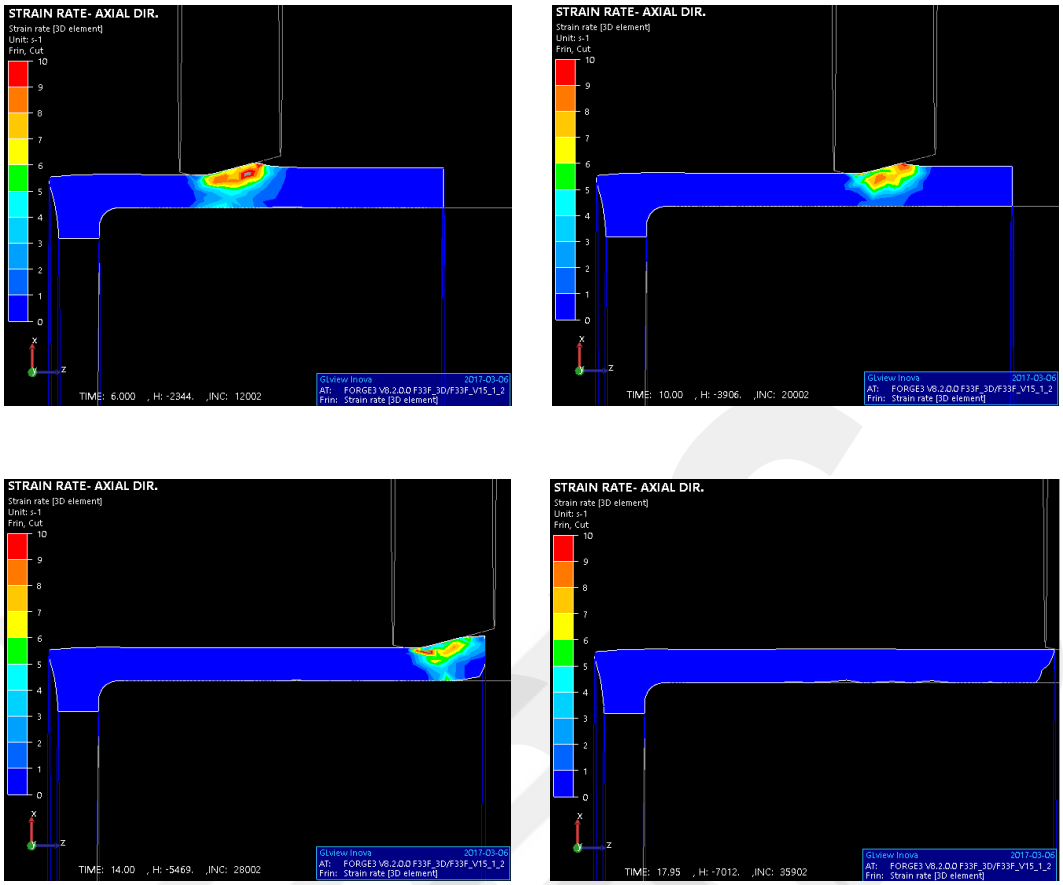

Figure 3.44 Strain rate distributions from different times

In the Figure 3.44, strain rate distributions has been shown at different time stages for tube spinning process. In the first picture, deformation can be penetrate up to the inner radius of the tube and localized at under right side of the roller and maximum at the contact zone. In the second picture, deformation is also localized under right side of the roller but penetration starts to move from inner radius to the surface of the tube because of this non homogeneous deformation along radial direction starts. At the third picture tube is deformed as non-homogeneously furthermore flaring occurs. The most important reason for flaring is deformation penetration zone starts to move along to the upper surface and upper surface deformation rate is more than the bottom surface. This situation creates a bending moment according to positive y axis and flaring occurs. Another reason is frictional force between contact surfaces. When enough forming force cannot be applied up to the inner radius of the tube, friction has been dominant and holds the material and elongation is slowing down at inner radius side. Forth picture is end of the tube spinning process. Because of the reasons explained in the third picture, non-homogeneous deformation, tube's end has an unstable edge. This instability is the nature of the tube spinning process end. Practically, by using second

tool at the end of the tube and instability can be minimized, but another tool cost will add to system. Generally, after the tube spinning process ends, the instable edge is cut, by doing this well flow formed product is obtained. In the picture below, 3D views of the tube spinning process can be seen, first one is at homogeneous deformation stage, tube's inner radius has full contact with the mandrel, and second one is nonhomogeneous deformation stage means at the end of the tube's inner surface contact between mandrel is lost and the flaring occurs.

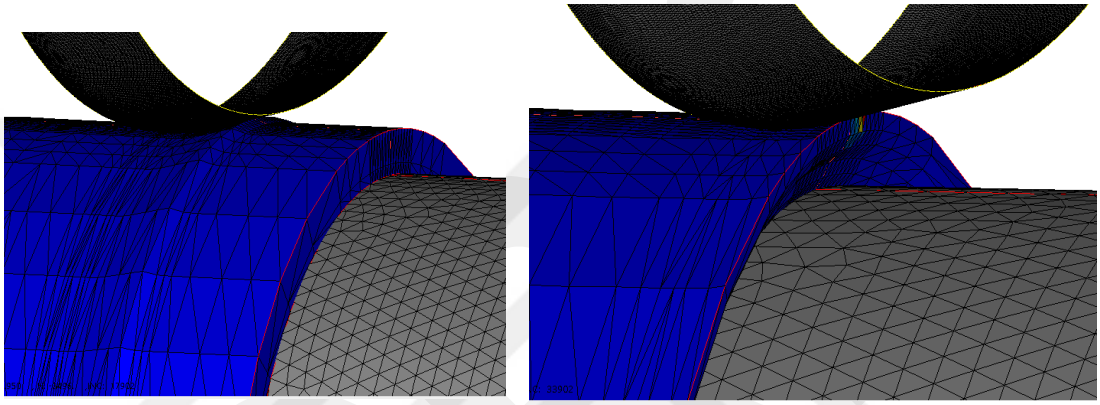

Figure 3.45 3D view of deformation at middle and end of the process

3.10 Von Mises Stress

During tube spinning process deformation occurs and continues at a certain area by localizing. In the figure above, axial and radial cross sections of a tube have been shown for the same time instance. Like the strain distribution, also von Mises stress distribution localizes. When looked from the axial cross sectional view, max von Mises stress is on the top surface of the spun tube and plastic deformation can penetrate up to the bottom surface. Von Mises values that are at localized deformation area under the roller, are higher than the yield stress, therefore that area deforms plastically and plastically deforming zones are colored above green legend, values under the green legend deform elastically.

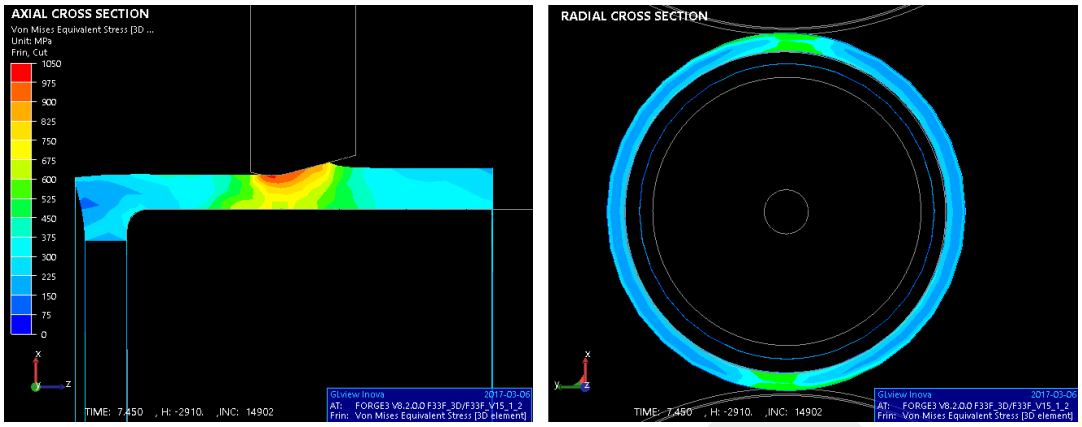

Figure 3.46 Von Mises stress distributions for axial and radial cross section

On the other hand, same situation with strain rate is also valid for von Mises stresses at radial cross section. Again a localized deformation zones occur under the roller and this zones take place right of the upper roller and left of the lower roller, this difference is related with the turning direction of the tube. Although deformation zones are at different sides of the roller, their distributions are absolutely have to be the same. When radial distribution of the von Mises stress is examined, it is obvious that, only the areas that under the roller, are deforming plastically, other circumferential zones are deforming elastically. Therefore, in the tube spinning process, the more rollers the tube spinning process has, the more plastically deformed areas it has.

During the process, plastic deformation has different distributions. The figure below for four different time interval axial cross sections are shown. At the beginning of the process plastic deformation occurs just under the roller and it can penetrate up to the inner radius of the tube. Moreover, the area that is front of the roller is plastically deformed up to the inner radius of the tube, as move away from the roller, von Mises' values are decreasing, it can be seen in the first picture of Figure 3.47, as distance increases from roller, legend turns from yellow to the green.

As the stroke of the roller increases, von Mises' distribution under the roller will not change, however, the distribution in front of the roller will change and it is not able to reach inner radius of the tube. Because of this situation, nonhomogeneous deformation starts at this stage. This is the starting point of flaring, top surface deforms but inner surface starts to behave elastically. Additionally, friction force holds the inner surface, therefore, inner surface cannot elongate along to the feeding direction.

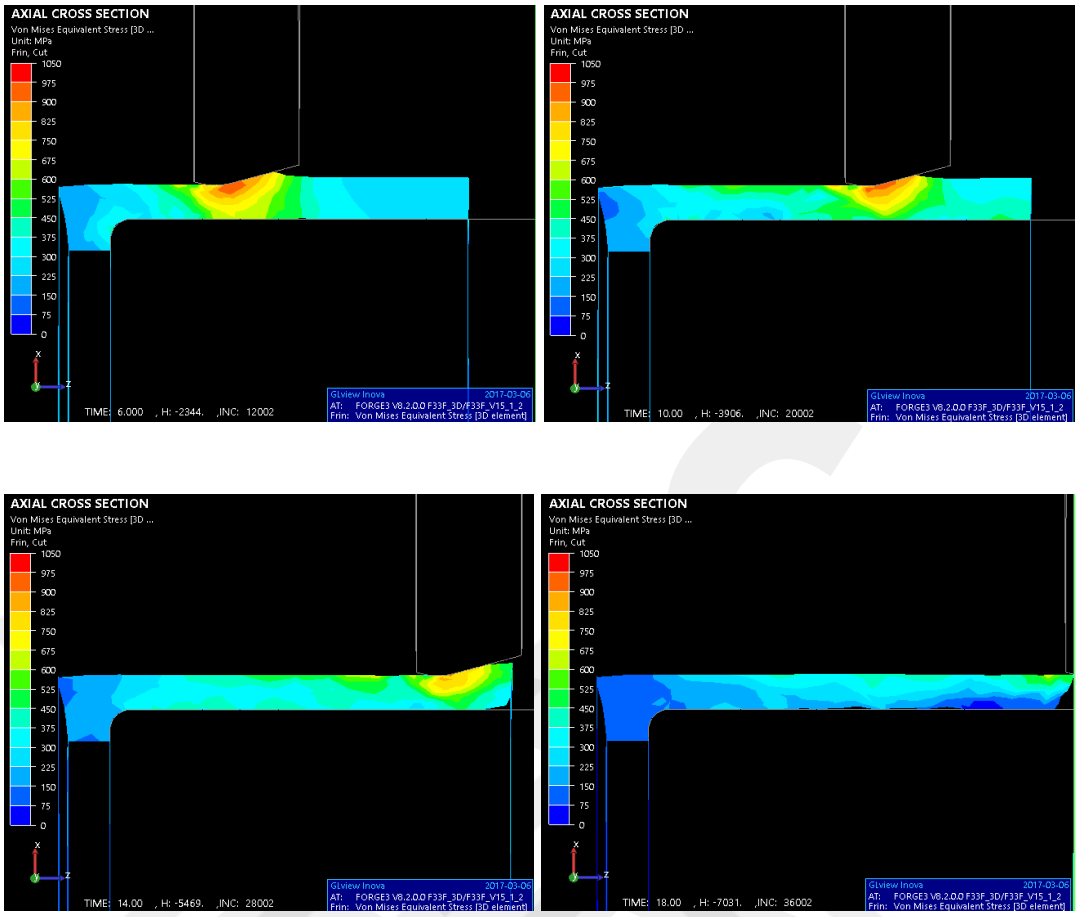

Figure 3.47 Von Mises stress distributions at different time stages

3.11 Hydrostatic Pressure

The hydrostatic pressure “p” is defined as one third of the trace of the stress tensor, that is, as the average of the diagonal terms:

$$p = -\frac{1}{3} tr([\sigma]) = -\frac{\sigma_{11} + \sigma_{22} + \sigma_{33}}{3}$$

Hydrostatic pressure shows the whether the areas are affected by compression or tension. Compression or tension situations are defined according to the pressure value; if the pressure value is positive; that area is under compression, if the pressure is negative, that area is under tension.

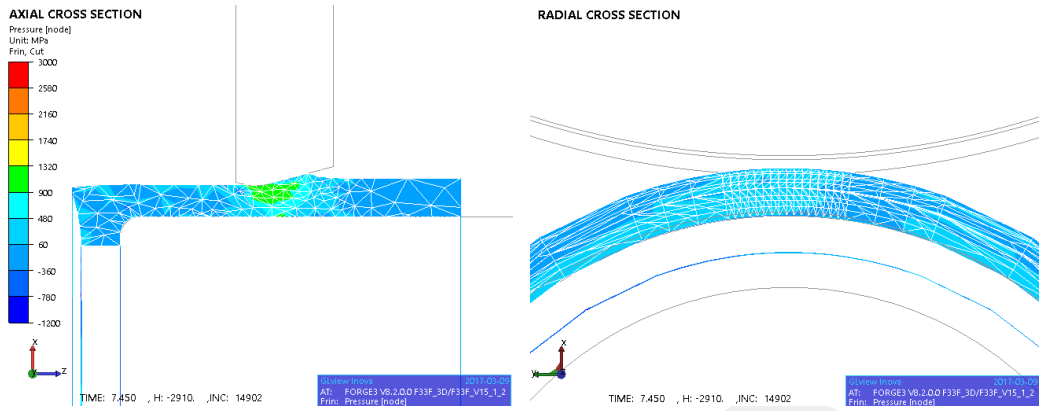

Figure 3.48 Hydrostatic pressure at axial and radial cross sections

Two cross sectional cut from both axial and radial directions is shown in the Figure 3.48 above. The area under the roller is affected as compression. Between midpoint of the thickness and outer surface of the tube is under more compression pressure than the area that is from midpoint to the inner radius. From axial cross sectional cut, it is seen that; compressive deformation localizes under the area where the roller and the tube have a contact, this situation again proves that during tube spinning process deformation is localized and it concentrates about just front, behind and under the roller. Other side of the tube, especially end of the tube affected by the tension. Formed area continues to the elongation.

When the legend is divided 3 section, areas that are affected from compressive and tension, can be observed easily;

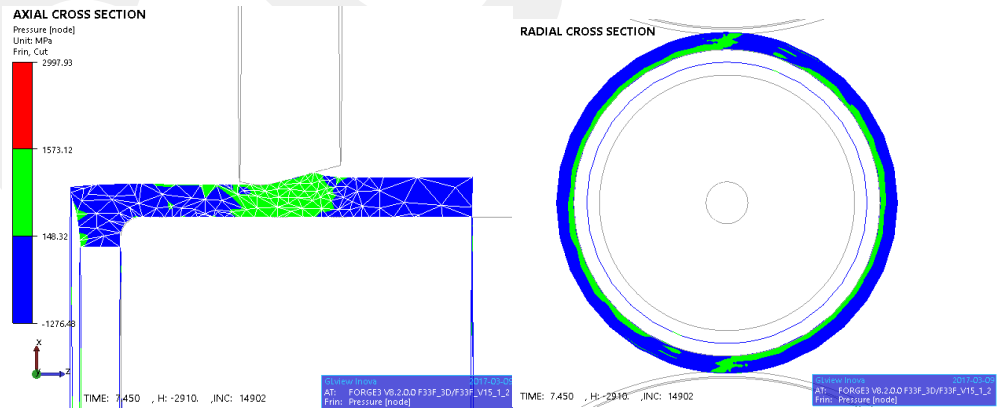

Figure 3.49 Three sectioned legend view of pressure

Tube‘s outer surface is under tension, and inner surface is under compression. However, under the rollers; compressive pressure can reach up to the inner surface of the tube. Radial force on the tube is along negative x axis, this means compressive.

3.12 Flaring Mechanism

By using tube spinning process, tubular workpiece's thickness can be decreased and length of the workpiece can be elongated. When thickness is reduced, material elongates along axial direction.

During process, elongation mechanism can be separated two section; that are uniform elongation and non-uniform elongation. Because of thickness reduction deformed material is piled up in front of the roller. Piled up material flows along axial direction and positive radial direction. Therefore, piled up section of the deformation has two different strain direction; one of them is along rolling direction other one is positive radial direction. Both of them is tensile strain. If material had been deformed along only rolling direction, there was no piled up material in front of the roller and tube's length just would only be elongated, moreover flaring would not be, like two dimensional tube spinning finite element deformation mechanism. During the formation of piled up material cylindrical strain gives information about deformation mechanism.

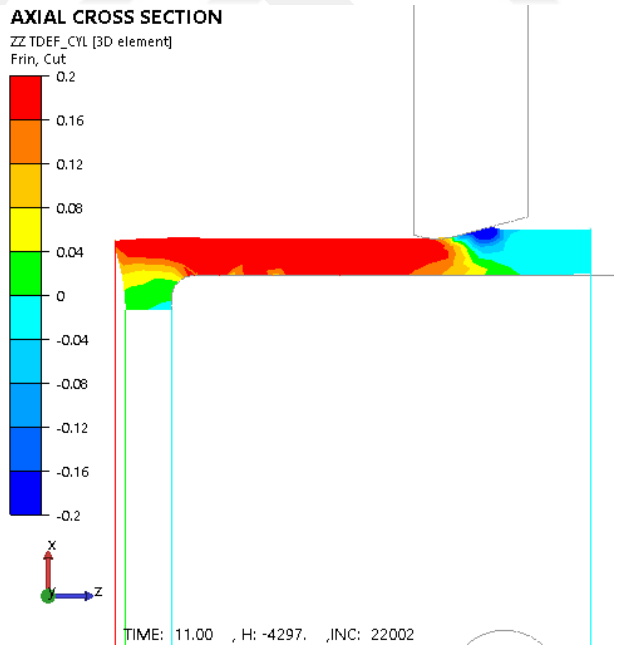

Figure 3.50 ZZ direction cylindrical strain

When Sze cylindrical strain tensor is examined along an axial cross section, the picture is unexpected. Under the roller tip radius, Strain values are positive and along the rolling direction and along the thickness it has same strain values. However, in front

of the roller deformation mechanism is different from under tip radius of roller. Cylindrical Sze direction strain values are positive at inner radius and cylindrical so strain values at piled up surface are negative. Formation direction of piled up material towards to opposite of rolling direction. In front of the roller's bottom side is deformed along positive z direction, outer surface of the front of roller is deformed along z direction and x direction. But strain rate of the x direction is faster than the z direction, therefore piled up material shrinks and draws the outside material along opposite side that is why flaring occurs during tube spinning process.

Actually, flaring always occurs during tube spinning process, but it can be observed just near the end of the process. At the beginning of the process flaring occurs but rest side of the tube holds the material. As the undeformed material size decreases, rest side of the material cannot hold the end of the tube and piled up material starts to pulling end of the tube towards to back and tube lose the contact with the mandrel and flaring occurs. Therefore, as tube length increases, formation of flaring will occur later than expected.
On the other hand, reduction of thickness amount also directly effects the formation of the flaring. For the tube spinning process, critical thickness reduction values are determined according to material and roller types. If unsuitable thickness reductions with roller and material type, unsteady states can be occur, moreover feeding rate is another reason of unsteady state tube spinning.

If the reduction ratio of the tube spinning process increases, flaring formation will be increases; means flaring will be occur earlier than the less reduction ratio. This situation can be explained with the XX cylindrical strain tensor. When the reduction ratios is increased, piled up material amount is increase and its height rises. In front of the roller piled up material's height rises because strain along XX direction grows up with increasing reduced thickness. Therefore when reduction ratio is increased, strain and strain rate will increase and formation time of flaring decreases and flaring occurs earlier.

Other factor that affects the flaring formation is used rollers' angles. Roller angle directly effects the piled up material's height. If the height of the piled up material increases, flaring formation risk increases. Because when the angle of the roller let

piled up material grow up along radial direction, flaring mechanism can be work easier and earlier. Furthermore, not only let the flaring but also unsteady state can be occur. Therefore, used roller's angle is absolutely important for a uniform elongation and steady state tube spinning.

3.13 Equivalent Strain Distribution

During tube spinning process, deformation is applied along 2 direction at the same time. Because of these deformation directions, tube's thickness is reduced and tube's length is increased. Therefore, large deformations occurs on the workpiece. The first aim for tube spinning is reducing the thickness and elongate the tube and the second aim is getting a strong cold formed product.

Equivalent plastic strain is denoted by $\bar{\varepsilon}$ and it is determined by the integration of the equivalent plastic strain rate as follows;

$$\bar{\varepsilon} = \int_0^t \dot{\bar{\varepsilon}} dt$$

Equivalent strain rate scalar can be used to highlight areas that have undergone a structural hardening. Strain hardening is expected at upper surface of the tube higher than the bottom side. Because large deformation occurs at outer surface of tube.

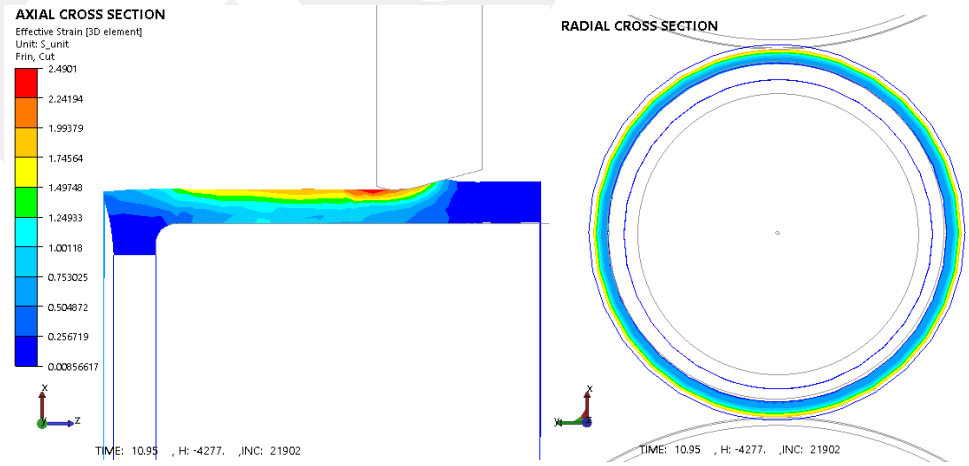

Figure 3.51 Equivalent strain at axial and radial cross sections

Outer surface of the tube is harder than the inner surface. As shown in the figure above, effective strain is greater at outer surface. However, it can reach nearly to the bottom

surface. Therefore, strain hardening situation can reach along radial direction and stiff parts can be achieved by using tube spinning process.

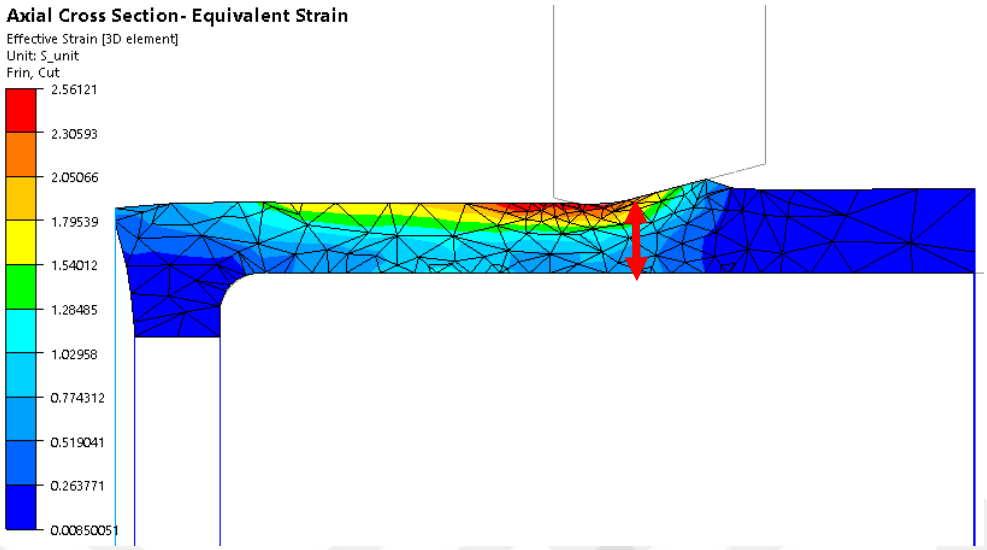

Figure 3.52 Equivalent strain at inner and outer surface of the tube

In the figure above, an axial cross section is shown. Dark red line are data points for effective strain. These data points are plotted as show in the below, length is distance from deformed outer surface of the tube. As going from outer surface to inner surface, effective strain values are decreasing;

Figure 3.53 Effective Strain along inner surface to outer surface of tube

3.14 Conclusion of Tube Spinning Mechanism

Tube spinning process has a complex stress state distribution. Process can be determined roughly with strain rate, von Mises distribution or equivalent strain, however, end of the process non uniform deformation and flaring mechanism are more complicated. Flaring mechanism can be explained with the cylindrical strain rate along axial direction. Inner surface of the tube has strain rate along positive axial direction but outer surface of the tube has a strain rate along negative axial direction, inner and outer surfaces deformation directions are different. Therefore in piled up material draw along opposite direction to rolling and bending occurs end of the tube and flaring starts.

4 CONCLUSION

Nowadays, special parts manufacturing is widely used in aviation, defiance and automotive industry. The prices of materials used during production are very high. On the other hand, it is highly profitable for firms to predict what the capacities of the machines will be for the production to be done. Because, initial investment of the tube spinning process machine are expensive. Therefore, according to material requirements, performing virtual experiments and simulations are beneficial for predicting to which machine capacity is needed and possibility about formability of the material and designed part.

Modelling and analyzing of tube spinning process needs high qualified and high capacity computers in order to make computation. Because, all meshed bodies in the model have rotational motion. Therefore, calculation time of the tube spinning process is higher than the other forming process. In order to reduce calculation time, two dimensional model can be used for virtual experiments. By using two dimensional model force and elongated length of the tube can be predicted. Deformation localizes under the rollers in tube spinning process. If the resultant force penetrates up to inner radius of the tube, length of the tube can be increased. Therefore, by analyzing, before doing experiments, it can be predicted that forces are enough to deform all material along thickness or not.

The tube spinning process has highly complex stress and strain distributions. In order to understand mechanism of the deformation, three dimensional model has to be used. Because, wave formation cannot be observed with two dimensional model. Also, wave formation in front of the roller directly effects the process mechanism. Strain rates gives information about the instantaneous deformation local zones. During the tube spinning process, maximum deformation occurs at the outer surface of the tube. Because of non- homogeneous deformation, as rollers come to end of the tube, discontinuity occurs and tube loses contact with mandrel. This situation is named as “flaring”. In order to observe flaring mechanism, three dimensional model has to be used.

5 RECOMMENDATIONS

During this thesis work lots of millstones is gained about tube spinning process finite element modelling. Used software is important. Because in tube spinning process all bodies have rotational motion, and they are under continuously changing contact conditions. Therefore computational time is more than the other forming process. Preparation of the three dimensional solid models of process tools should be done with highest possible accuracy as the tools are exported in STL format. This is because Transvalor Forge meshes the tools based on the imported STL file. The more accurate the STL format, the the more accurate the mesh becomes. On the other hand, rollers', mandrel's, tube's center point should be defined accurately. Because all of them have rotational motion, if centers are determined incorrectly, tools with rotate off-center and the analysis may not converge. Other important point is the mesh size. According to reduction ratio and thickness of the tube mesh size computational time study has to be done with a sectioned or shortened model, otherwise analysis will continue more than 20 days. The last thing is that results will be calculated by Transvalor Forge during the analysis only. Therefore, the user has to define all output results before running the analysis.

REFERENCES

[1] C.C.Wong , T.A. Dean, J.Lin, ‘A rewiev of spinning shear forming and flow forming process’, International Journal of Machine Tools and Manufacture, volume 43, pages 1419-1435, November 2003

[2] R.P. Singhal, S.R. Das, ‘Some experimental observations in the shear spinning of long tubes’, Journal of Mechanical Working Technology, volume 14, pages 149-157, 1987

[3] K.S. Lee, L.Lu, ‘A study on the flow forming of cylindrical tubes, Journal of Material Processing Technology’, volume 113, pages 739-742, June 2001

[4] M.Hayama, H. Kudo, ‘Experimental study of tube spinning’, The Japan Society of Mechanical Engineers, volume 22, pages 769-775, May 1979

[5] P.Groche, D. Fritsche, ‘Application and modelling of flow forming manufacturing processes for internally geared wheels’, International Journal of Machine Tools and Manufacture, volume 46, pages 1261-1265, September 2006

[6] M.J. Roy, D.M. Maijer, R.J. Klassen, J.T. Wood, E. Schost, ‘Analytical solution of the tooling/workpiece contact interface shape during a flow forming operation’, Journal of Material Processing Technology, volume 14, pages 1976-1985, November 2010

[7] Y. Xu, S. H. Zhang, P. Li, K. Yang, D. B. Shan, Y. Lu, ‘3D rigid-plastic FEM numerical simulation on tube spinning’, Journal of Material Processing Technology, volume 113, pages 710-713, June 2001

[8] H. Lexian, B.M. Dariani, ‘An analytical contact model for finite element analysis of tube spinning process’, Journal of Engineer Manufacture, pages 1375-1385, July 2008

[9] C.C. Wong a, J. Linb, T.A. Deanb, ‘Effects of roller path and geometry on the flow forming of solid cylindrical components’, Journal of Materials Processing Technology, volume 167, pages 344-353, 2005

[10] F.A. Hua, Y.S. Yang, Y.N. Zhang, M.H. Guo, D.Y. Guo, W.H. Tong, Z.Q. Hu, ‘Three-dimensional finite element analysis of tube spinning’, Journal of Materials Processing Technology, volume 168, pages 68-74, September 2005

[11] Z. Handong, Z.Hua, Z.Chongyang, ‘The analysis of tube spinning process parameters on workpiece defects ‘, Manufacturing Science and Technology, International Conference on Advanced Engineering Materials and Technology (AEMT 2011, Sanya, China), pages 1656-1659, July 2011,

[12] Z.Y. Zhao, S.J. Tu, R.Y. Zhang, Z.H. Guo, J.H. Cui, ‘Influence of wall thinning rate on bell mouth defect during hot power backward spinning for casting aluminum alloy tube’, Journal of Plasticity Engineering, Volume 21, pages 116-120, 2014

[13] H. Ma, W. Xu, B.J. Jin, D.Shan, S.N. Nutt, ‘Damage evaluation in tube spinnability test with ductile fracture criteria’, International Journal of Mechanical Sciences, Volume 100, pages 99-111, September 2015

[14] M.Runge,"Spinning and Flow forming‖, (D.H. Pollitt, Trans) Lei-field GmbH, Werkzeugmaschinenbau/Verlag Moderne Industrie AG, D-86895, Landsberg/Lech, 1994